Michelangelo Merisi da Caravaggio, Narcisse

Изучение поверхностей с помощью рентгеновской рефлектометрии и дифракции в скользящей геометрии

Oleg Konovalov
ESRF / ID10B

Outlook

1. Introduction
2. Surface sensitivity
3. Theory and Applications of
   - X-ray reflectivity
   - Diffuse scattering
   - Grazing Incidence Diffraction
   - Grazing Incidence Small Angle Scattering
   - Total Reflection X-Ray Fluorescence
4. Conclusions

Зачем изучать поверхности ?

? **фазовые границы раздела**

? **рост кристаллов**

? **химические реакции на поверхностях**
   ⇨ катализ

? **физика двумерных систем**

? **тонкие пленки, мембраны**

? **....**

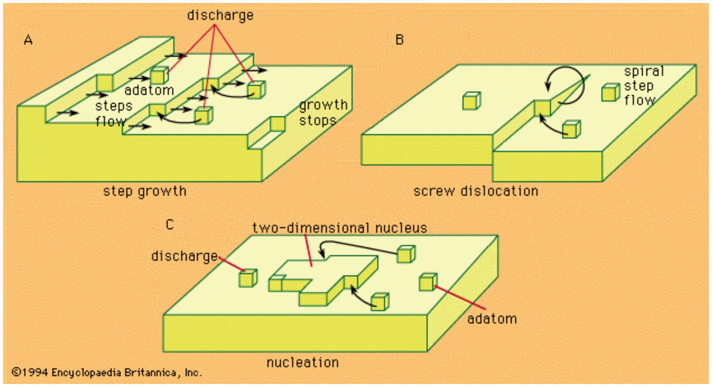

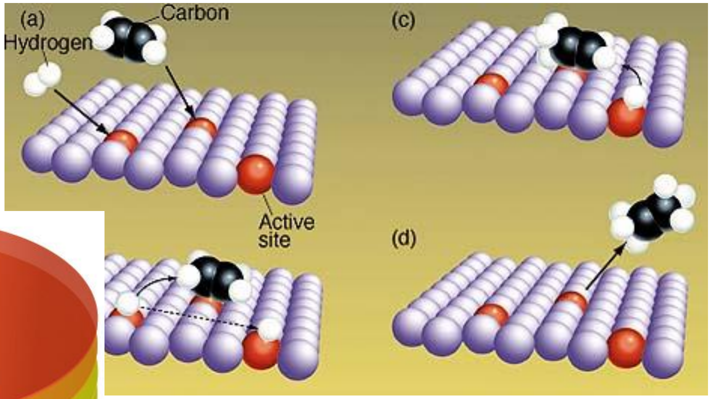

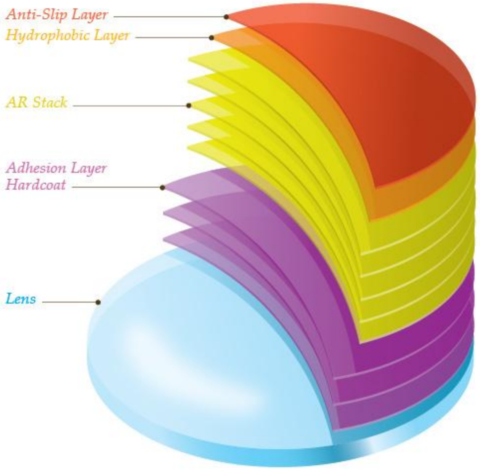

Scientific Applications

- Surface structure of simple and complex fluids (colloid, gel, sol,…)
- Langmuir films, amphiphilic polymers and nano- particle at the air-water interface
- Capillary wave and surface roughness
- Structure and growth of two dimensional crystals of molecules, macromolecules and proteins
- Morphology and crystalline structure of thin organic and non-organic films on solid substrates
- Phenomena at liquid/liquid and solid/liquid interfaces
- Cell membranes
- Shape, strain, ordering and correlation of crystalline nanostructures, quantum dots and wires on substrates

How to study surfaces and interfaces ?

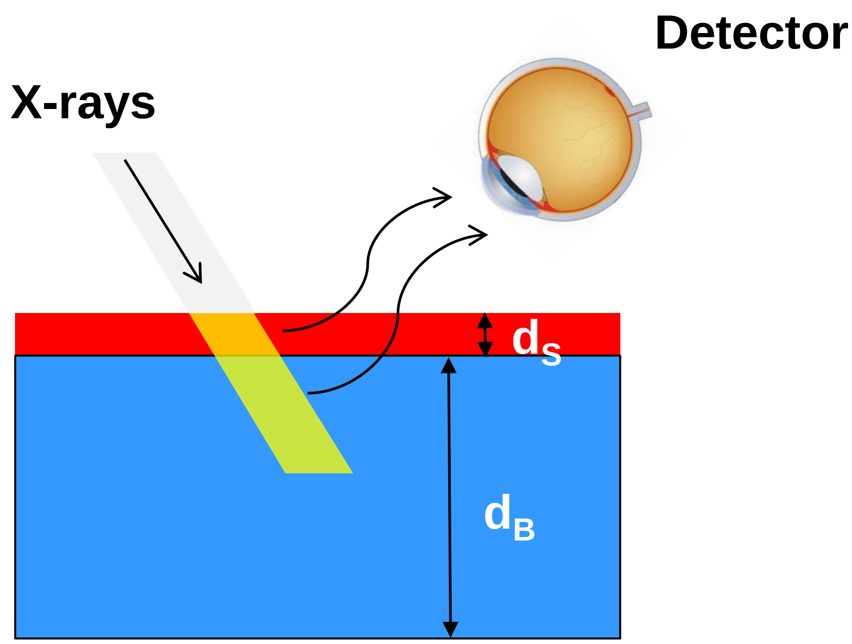

$$I(\vec{q}) = \left| \sum_{k}^{N} f_k \exp\left(-i \cdot \vec{q} \cdot \vec{r}_k\right) \right|^2$$

$$I \sim N \cdot f^2 = \left(N_S + N_B\right) \cdot f^2$$

$$\frac{I_S}{I_B} = \frac{N_S}{N_B} = \frac{d_S}{d_B}$$

$$\frac{I_S}{I_B} = \frac{100\,nm}{100\,\mu m} = \frac{10^{-7}}{10^{-4}} = 10^{-3}$$

Surface Sensitivity

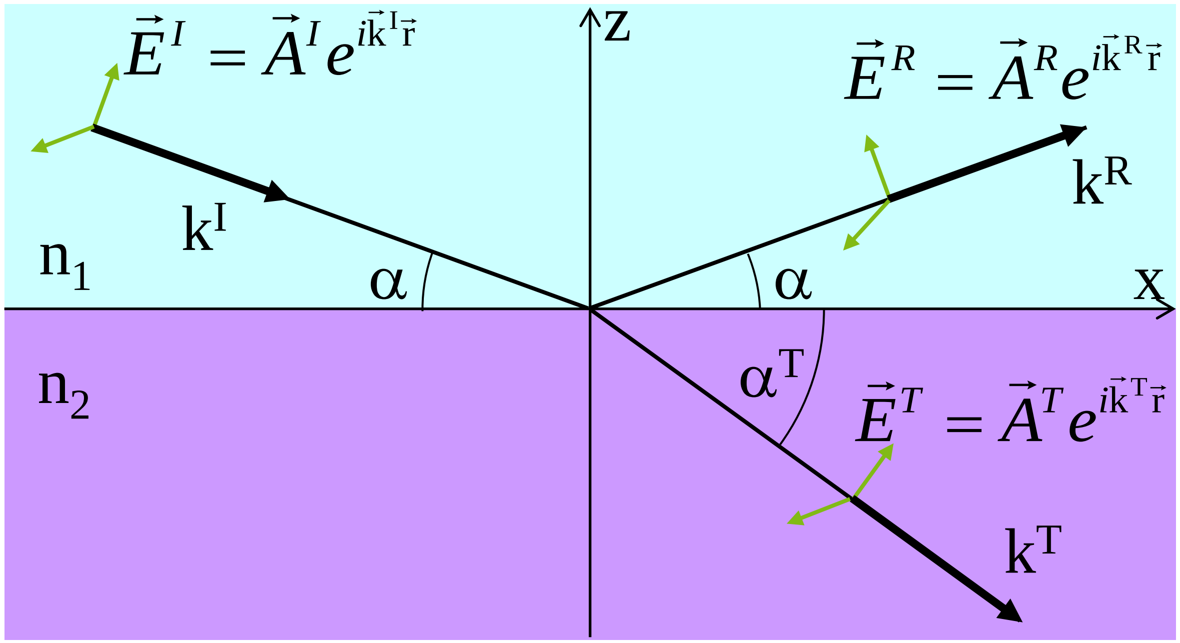

Wave and its derivative are continuous at z=0

$$A^I + A^R = A^T$$

$$A^I \vec{k}_I + A^R \vec{k}_R = A^T \vec{k}_T$$

$$k = \left|\vec{k}_I\right| = \left|\vec{k}_R\right| \qquad nk = \left|\vec{k}_T\right|$$

$$\frac{\cos\alpha}{\cos\alpha^T} = \frac{n_2}{n_1} = n$$

For X-rays: $n = 1 - \delta - i\beta$ $\quad \delta = \frac{\lambda^2 r_e}{2\pi}\rho_{el}$ $\quad \delta \sim 10^{-6}$ $\quad |n| < 1$ $\quad \alpha_c \sim \sqrt{2\delta}$

$$\alpha^T = \mathrm{Re}\left(\alpha^T\right) + i \cdot \mathrm{Im}\left(\alpha^T\right)$$

$$\beta = \frac{\mu\lambda}{4\pi}$$

Intensity falls off with 1/e penetration depth Λ

$\perp$ - component $\quad A^T e^{i\left(k\alpha^T\right)z} = A^T e^{ik\,\mathrm{Re}\left(\alpha^T\right)z}\, e^{-k\,\mathrm{Im}\left(\alpha^T\right)z}$

$$\Lambda = \frac{1}{2k\,\mathrm{Im}\left(\alpha^T\right)}$$

Surface Sensitivity

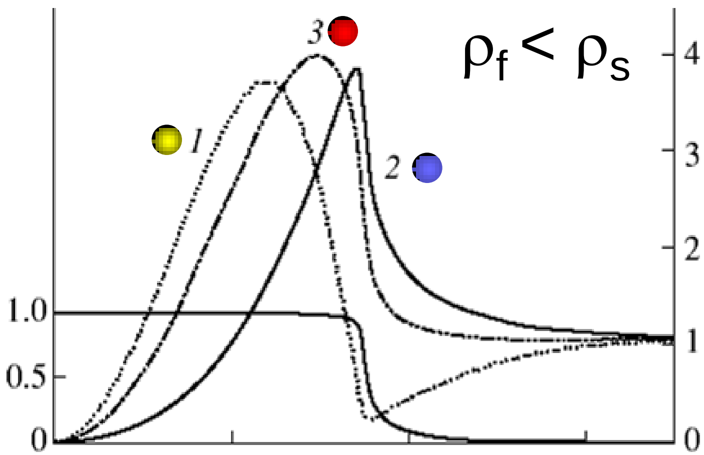

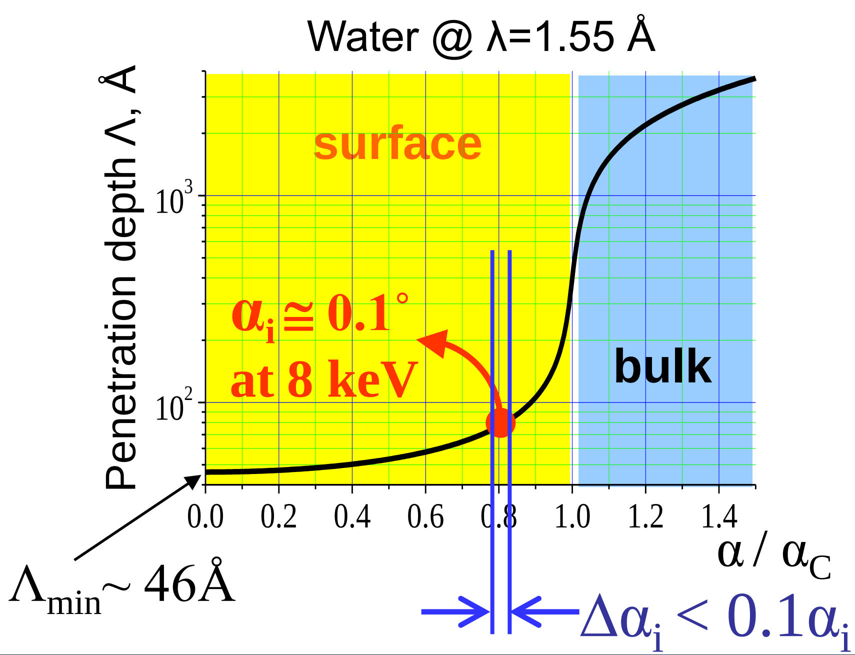

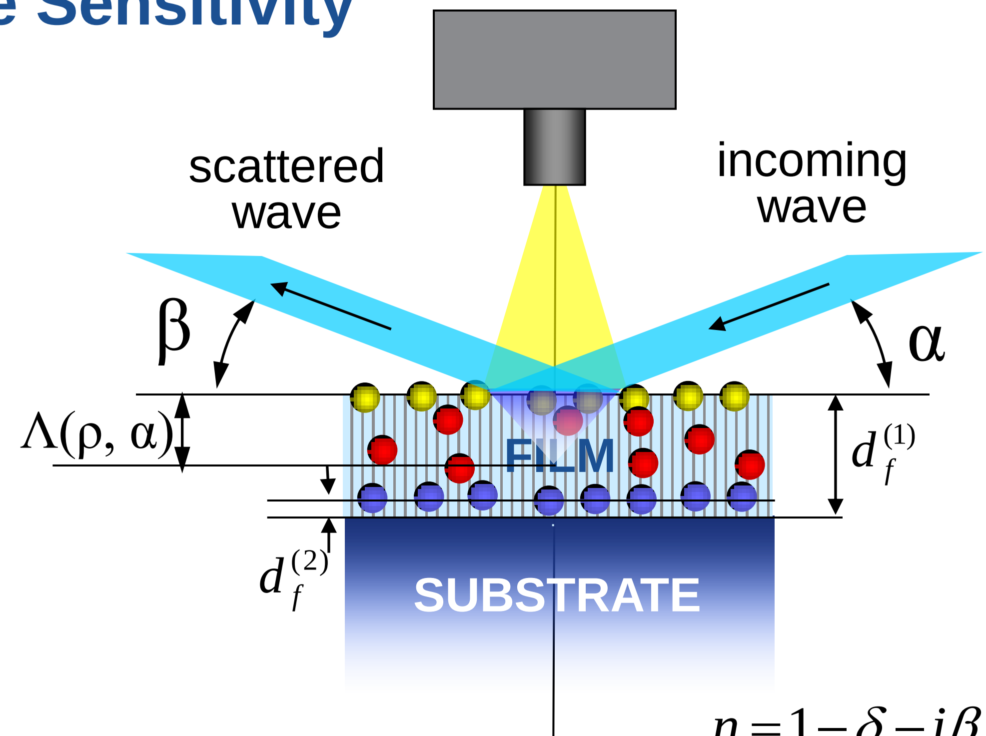

$$n = 1 - \delta - i\beta$$

$$\delta = \frac{\lambda^2 \rho r_e}{2\pi} \qquad \delta \approx 10^{-6} \qquad \alpha_c = \sqrt{2\delta} \qquad \alpha_C \sim \text{mrad}$$

$$\Lambda(\alpha) = \frac{\lambda}{2\sqrt{2}\pi\left(\sqrt{\left(\alpha^2 - \alpha_C^2\right) + 4\beta^2} - \sqrt{\left(\alpha^2 - \alpha_C^2\right)}\right)^{1/2}}$$

$$\text{if } \alpha < \alpha_c\,,\ \Lambda = \left(q_c\sqrt{1 - \left(q/q_c\right)^2}\right)^{-1}$$

Surface Scattering Techniques

XR
X-ray Reflectivity (α=β, γ =0)
In-depth electron density profile – thickness, density and roughness of films

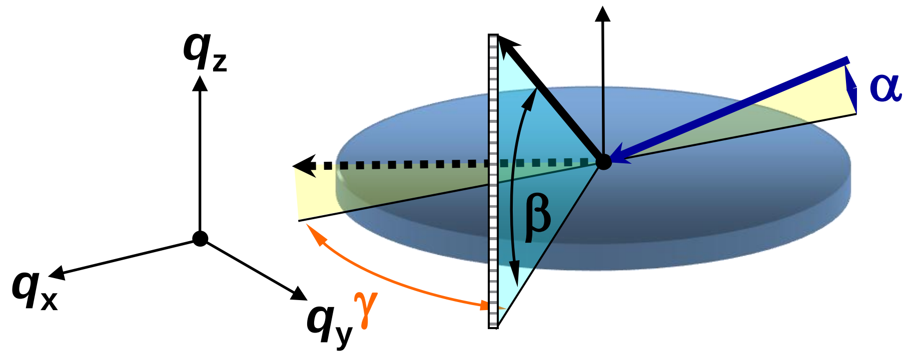

GISAXS
Grazing Incidence Small-Angle X-ray Scattering ($\alpha < \alpha_c$, $\gamma \geq 0$, $\beta \geq 0$)
Particle geometry, size distributions and spatial correlations on nanometer scale

GID
Grazing Incidence Diffraction ($\alpha < \alpha_c$, $\gamma \geq 0$, $\beta \geq 0$)
Two dimensional crystals (lattice parameters, molecular structure, tilt angle of molecules, in-plain correlation lengths

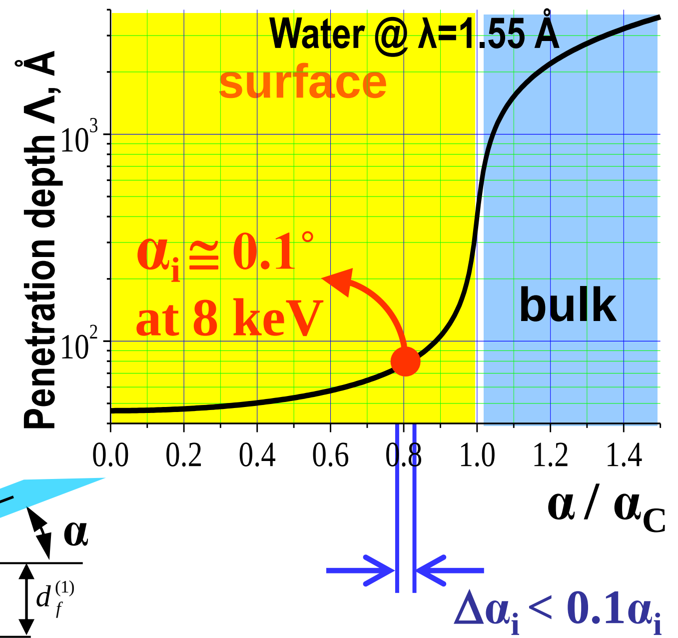

GIXF
Grazing Incidence X-ray Fluorescence ($\alpha < \alpha_c$, $\gamma = 90°$)
In-depth elemental distribution profile

$$q = \frac{2\pi}{\lambda} \begin{Bmatrix} \cos\beta\cos\gamma - \cos\alpha \\ \cos\beta\sin\gamma \\ \sin\beta + \sin\alpha \end{Bmatrix}$$

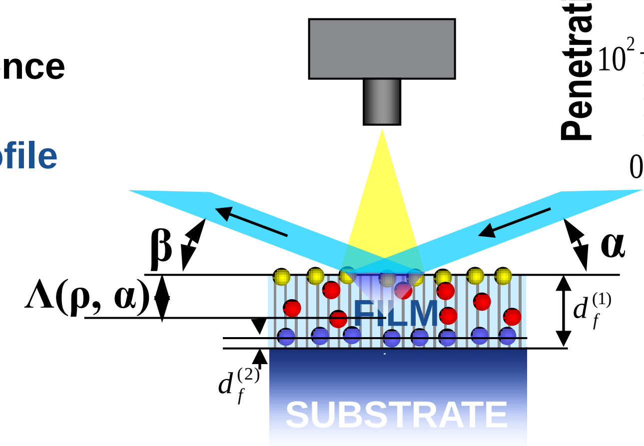

Cell Membrane ⇔ Surface Scattering Methods

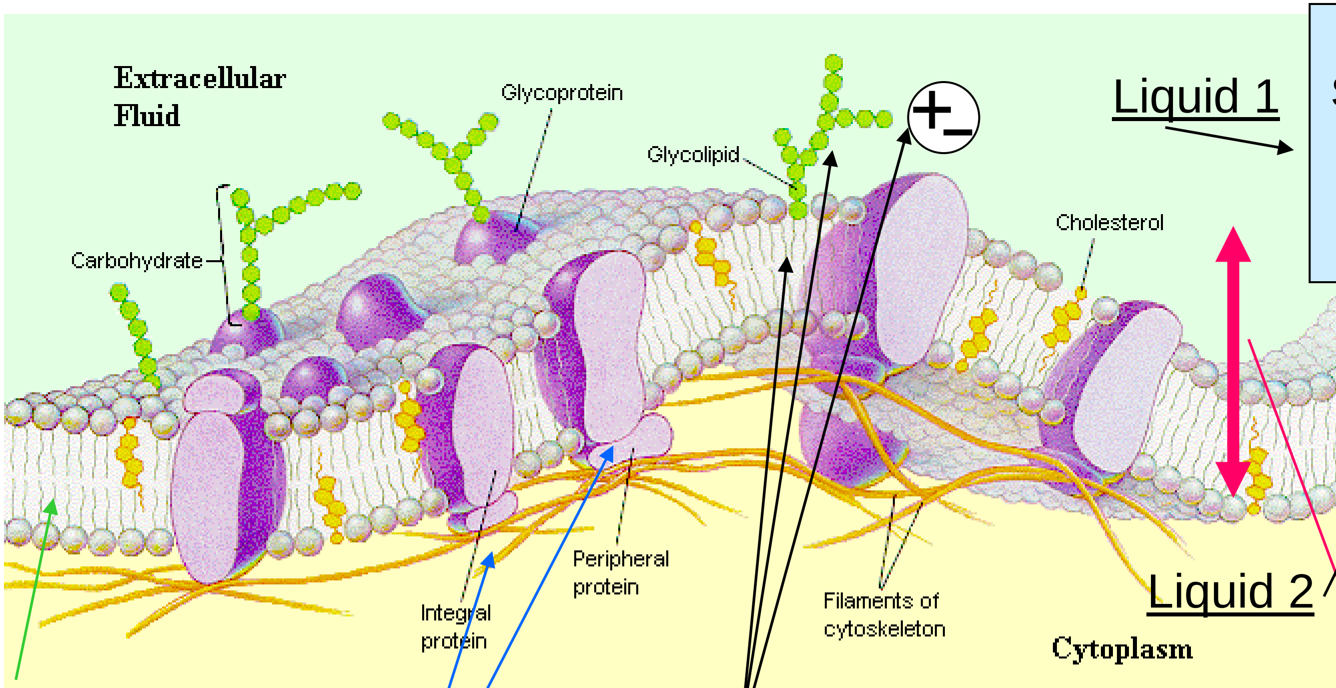

Environment & Surface energy Control
⇩
High energy

GID
⇩
Lipids matrix organization

GISAXS
⇩
Protein organization
(*dilute, condensed and crystalline*)

Reflectivity + Fluorescence
⇩
Electron density & ions distribution
Membrane interaction with molecules and macromolecules

GI Diffuse Scattering
⇩
Membrane fluctuation and elastic properties

Surface scattering on membranes mimicked with Langmuir method

sample molecules in solvent

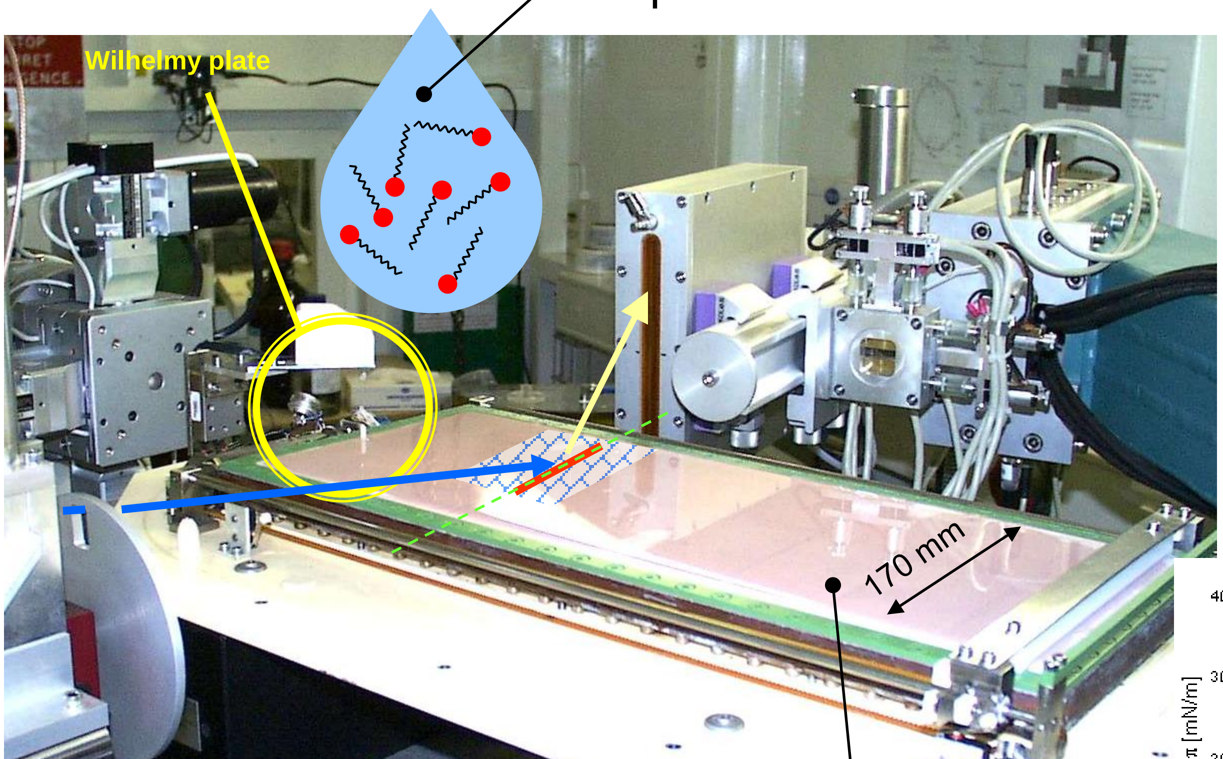

Control
area per molecule
(i.e. surface pressure)
temperature

phase transition:
gas – liquid – crystal

α_i=2 mrag
foot print at 100 μm beam is 50 mm

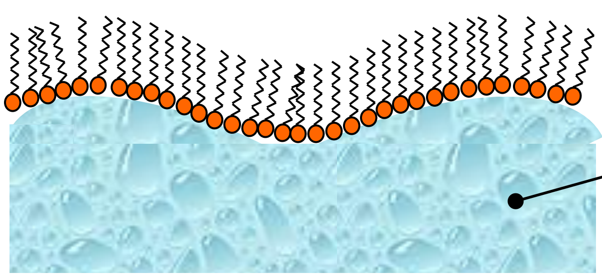

subphase
(water)

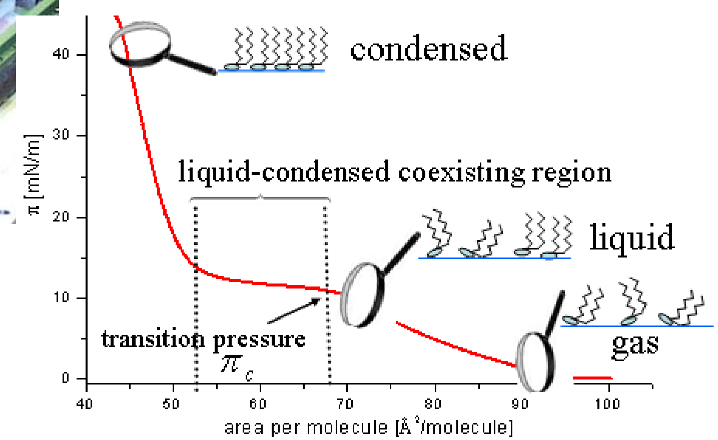

Рентгеновская Рефлектометрия

X-Ray Reflectivity

Fresnel Formulas

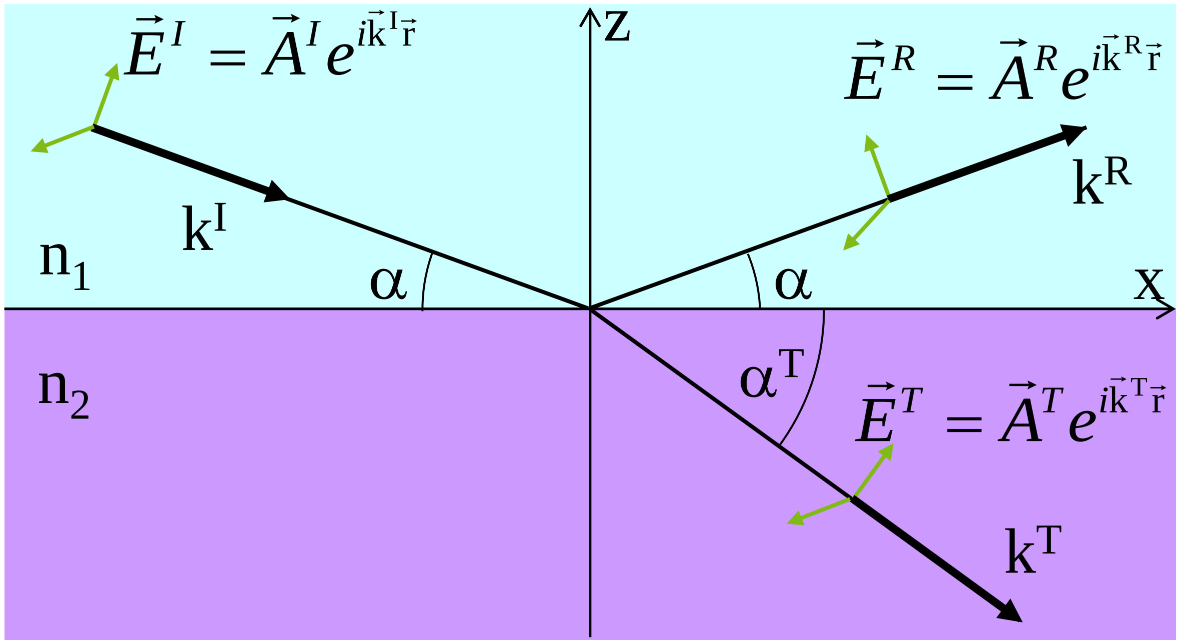

Wave and its derivative are continuous at z=0

$$A^I + A^R = A^T$$

$$A^I \vec{k}_I + A^R \vec{k}_R = A^T \vec{k}_T$$

$$k = \left|\vec{k}_I\right| = \left|\vec{k}_R\right| \qquad nk = \left|\vec{k}_T\right|$$

$$\frac{\cos\alpha}{\cos\alpha^T} = \frac{n_2}{n_1} = n = 1 - \delta - i\cdot\beta$$

$$r_\perp = \frac{A_\perp^R}{A_\perp^I} = \frac{n_1\sin\alpha - n_2\sin\alpha^T}{n_1\sin\alpha + n_2\sin\alpha^T} = \frac{\sin\alpha - \sqrt{n^2 - \cos^2\alpha}}{\sin\alpha + \sqrt{n^2 - \cos^2\alpha}} \approx \frac{\sin\alpha - \sqrt{\sin^2\alpha - 2\delta}}{\sin\alpha + \sqrt{\sin^2\alpha - 2\delta}}$$

$$t_\perp = \frac{A_\perp^T}{A_\perp^I} = \frac{2n_1\sin\alpha}{n_1\sin\alpha + n_2\sin\alpha^T}$$

$$r_\parallel = \frac{A_\parallel^R}{A_\parallel^I} = \frac{n_2\sin\alpha - n_1\sin\alpha^T}{n_2\sin\alpha + n_1\sin\alpha^T}$$

$$t_\parallel = \frac{A_\parallel^T}{A_\parallel^I} = \frac{2n_1\sin\alpha}{n_2\sin\alpha + n_1\sin\alpha^T}$$

$$2\delta = \sin^2\alpha_c$$

$$\alpha_c \approx \sqrt{2\delta} = \sqrt{\pi^{-1}\lambda^2 r_e \rho_{el}}$$

Reflectivity from homogeneous layer

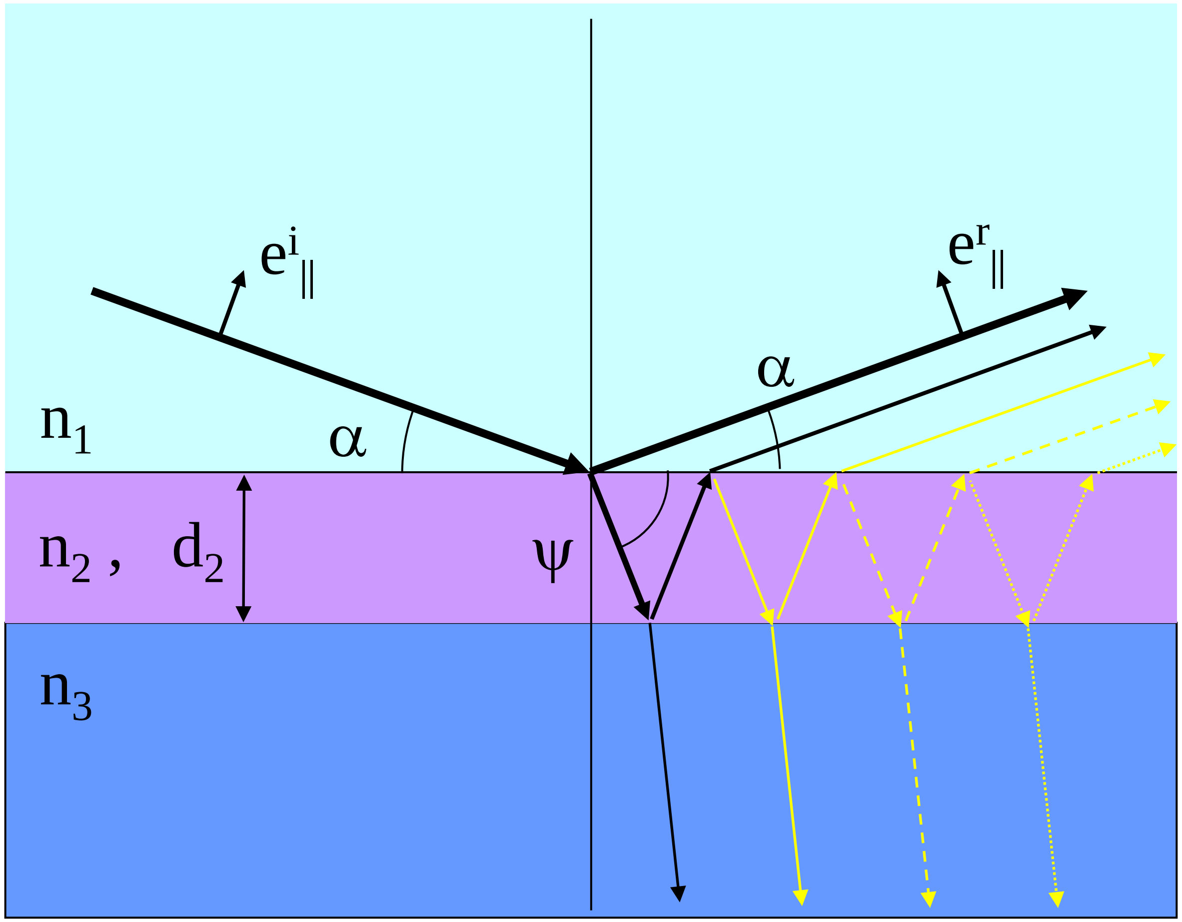

$$r_\perp^{1,2} = \frac{n_1 \sin\alpha - n_2 \sin\psi}{n_1 \sin\alpha + n_2 \sin\psi}$$

$$r_\perp^{eff} = \frac{r_\perp^{1,2} + r_\perp^{2,3} X}{1 + r_\perp^{1,2} r_\perp^{2,3} X}$$

$$X = e^{-\frac{i 4\pi d_2 n_2 \sin\psi}{\lambda}}$$

Typical Examples of Reflectivity Curves

air/water interface

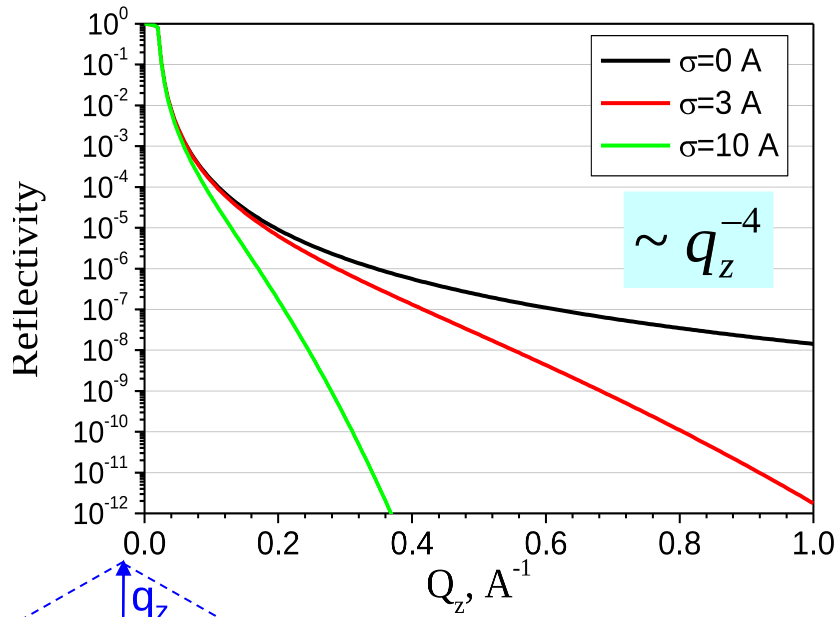

film on water (thickness d=20A)

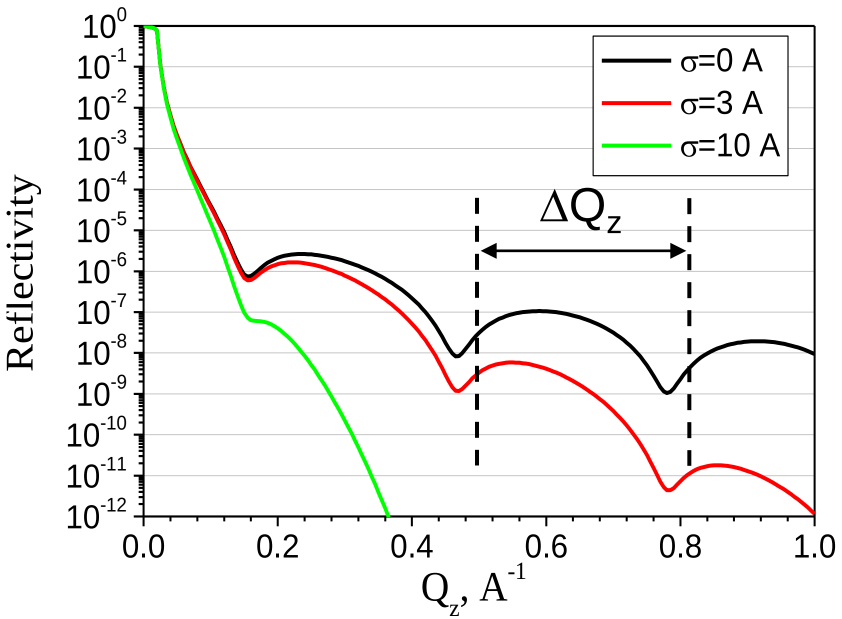

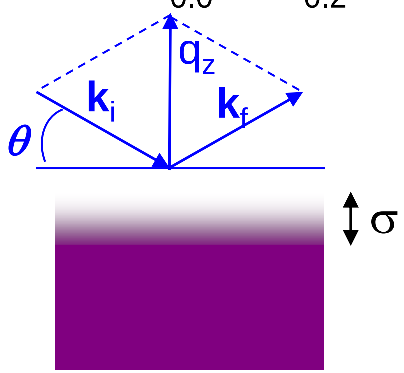

$$q_z = \frac{4\pi}{\lambda}\sin\theta \qquad F_{1,2} = \frac{\eta_1 - \eta_2}{\eta_1 + \eta_2}$$

$$\eta_j = \sqrt{\sin^2\theta - 2(\delta_j + i\beta_j)}$$

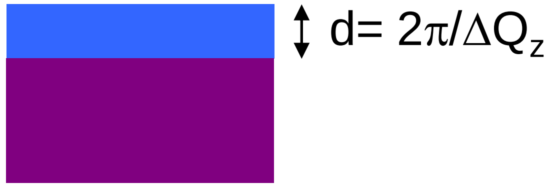

Roughness and specular reflectivity limitation

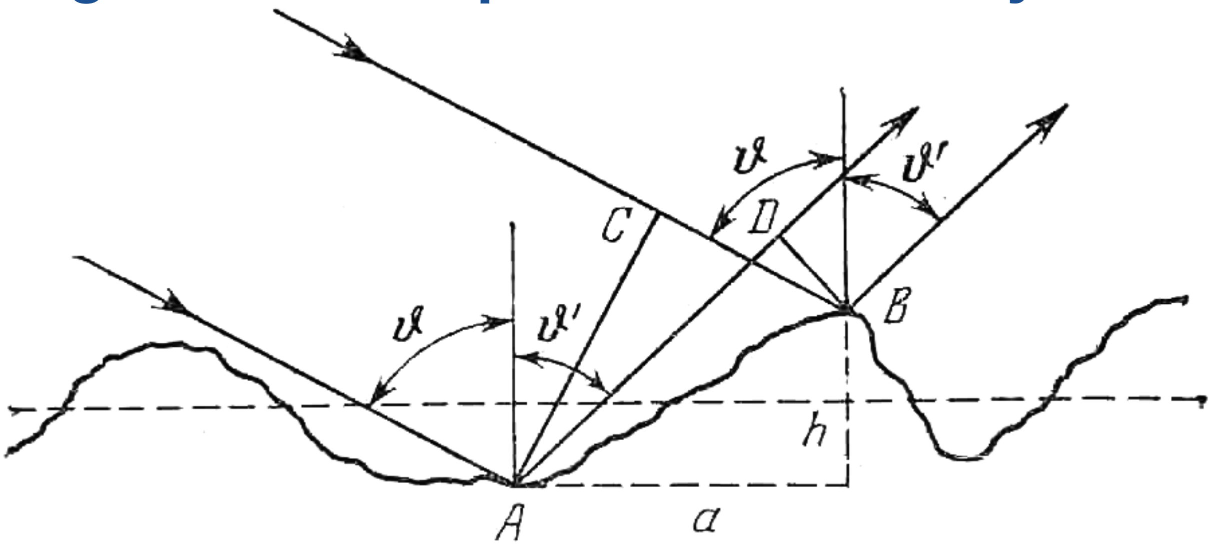

$$\Delta = AD - BC = a(\sin\vartheta' - \sin\vartheta) + h(\cos\vartheta' + \cos\vartheta)$$

$$\vartheta' = \vartheta \qquad \Delta = 2h\cos\vartheta \qquad \theta = \pi/2 - \vartheta$$

$$\Delta = 2h\sin\theta \quad \langle\langle \lambda \quad \le \lambda / n \rightarrow \quad \sin\theta = \frac{\lambda}{2nh}$$

$$q_z^{\max} = \frac{4\pi}{\lambda}\sin\theta_{\max} = \frac{2\pi}{nh} \approx 0.52\,A^{-1} \quad / \, at\ n = 4\ \&\ h = 3A$$

Roughness and specular reflectivity limitation

air/water interface

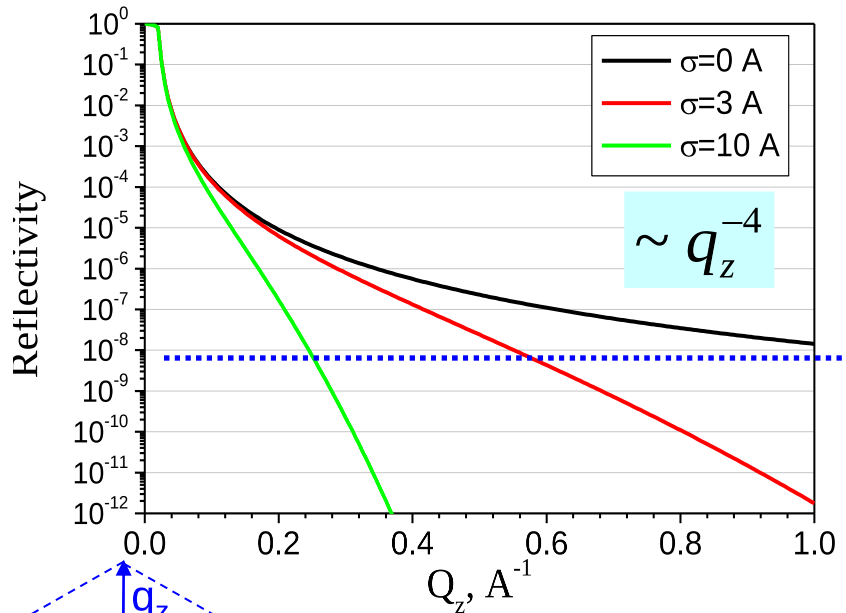

film on water (thickness d=20A)

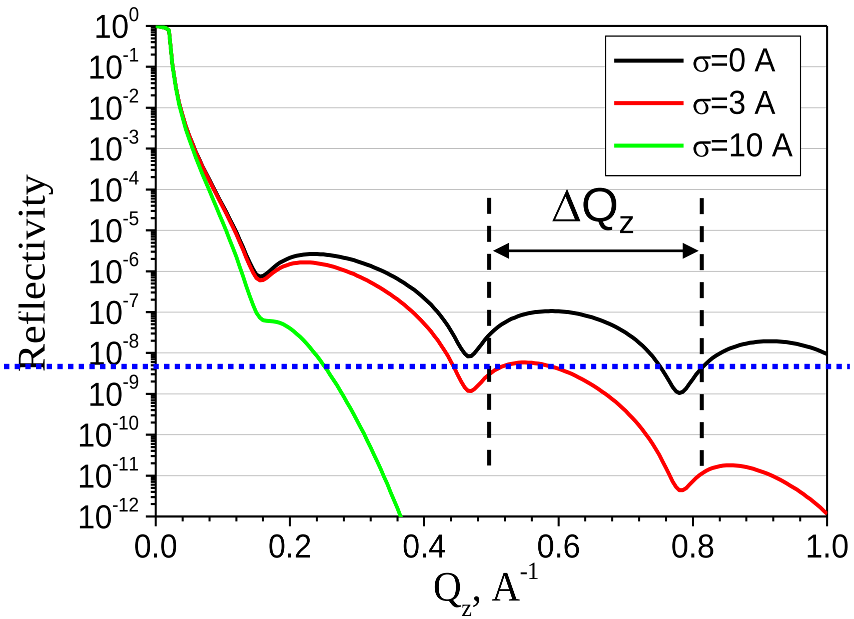

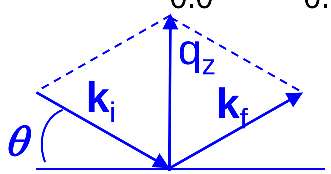

$$q_z = \frac{4\pi}{\lambda}\sin\theta \qquad F_{1,2} = \frac{\eta_1 - \eta_2}{\eta_1 + \eta_2}$$

$$\eta_j = \sqrt{\sin^2\theta - 2(\delta_j + i\beta_j)}$$

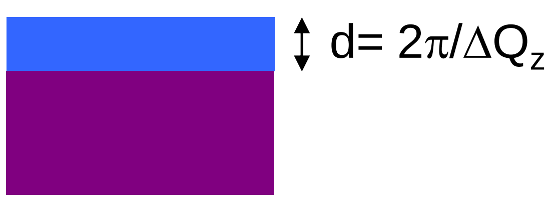

Reflectivity calculation *(Parratt version)*

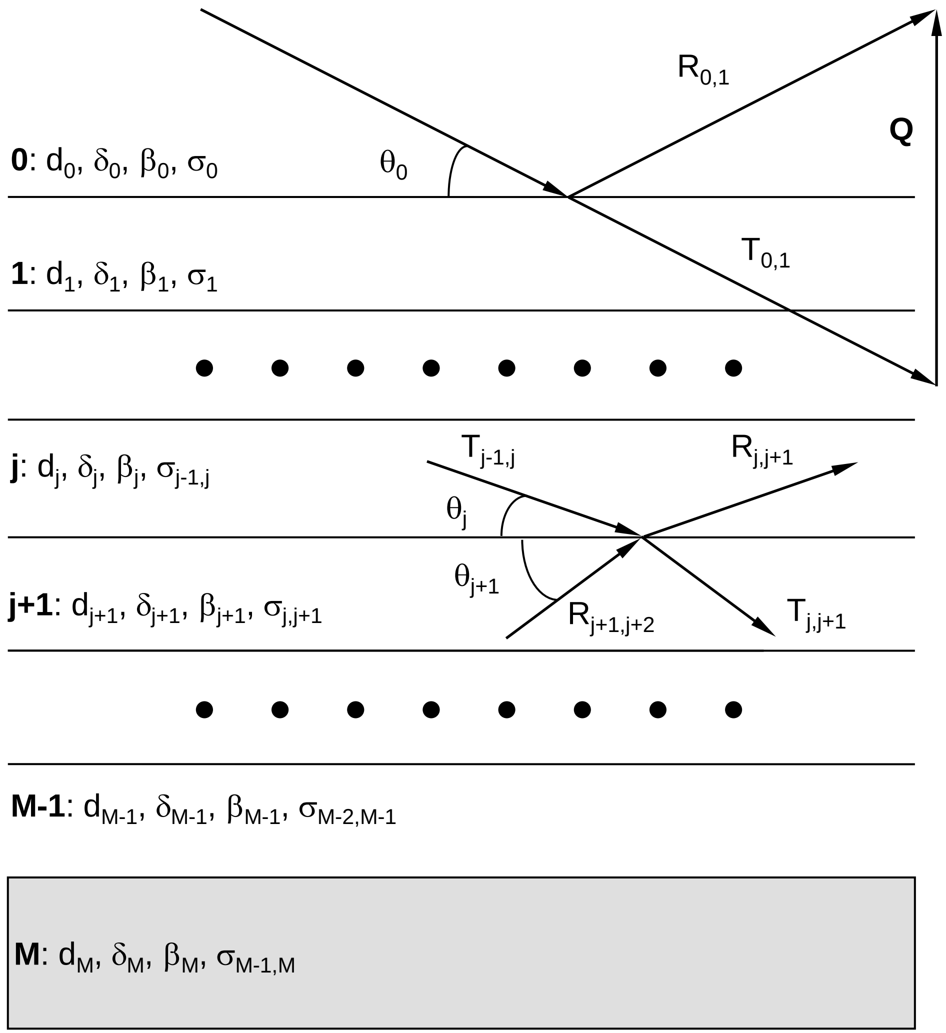

Reflectivity is $I(q)=|R_{0,1}(q)|^2$, where $R_{0,1}(q)$ is calculated from recursive formula

$$R_{n-1,n} = a_{n-1}^4 \cdot \left| \frac{R_{n,n+1} + F_{n,n-1}}{1 + R_{n,n+1} F_{n-1,n}} \right|$$

$R_{n,n+1}=a_n^2 \times E_n^R/E_n$,
$F_{n-1,n}=(\eta_{n-1}-\eta_n)/(\eta_{n-1}+\eta_n)$,
$\eta_n=(N_n^2+\cos^2(\theta))1/2$,
$a_n=\exp(-ik\eta_n d_n/2)$,
$n=0,1,2,\ldots,M$; $k=2\pi/\lambda$,
λ- wave length,
E_n , E_n^R –amplitudes of transmitted and reflected fields in the layer n,
d_n – thickness of layer n, material index $N_n=1-\delta_n-i\times\beta_n$;
n=M for substrate,
$R_{M,M+1}=0$.

Parratt L.G. Physical Review., 1954, v.95, p.359

X-ray Reflectivity Principle

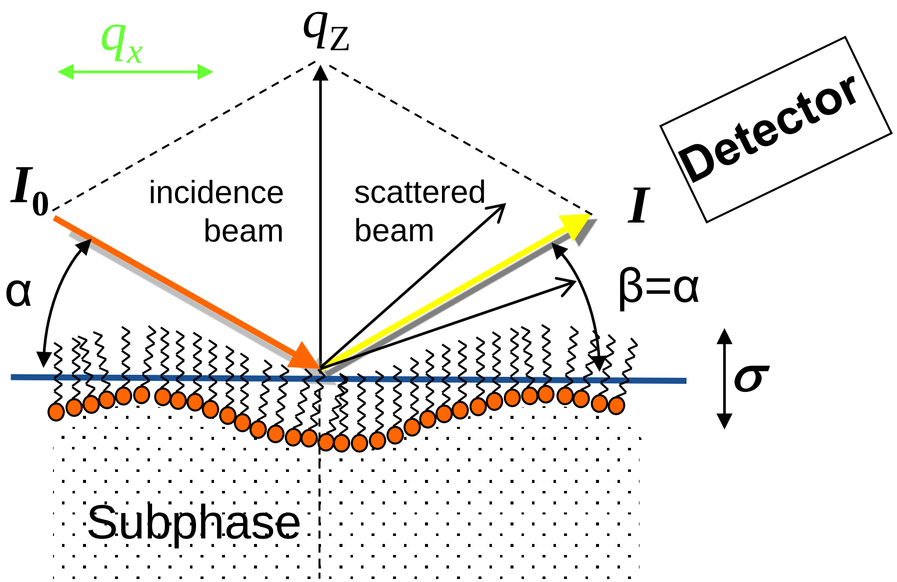

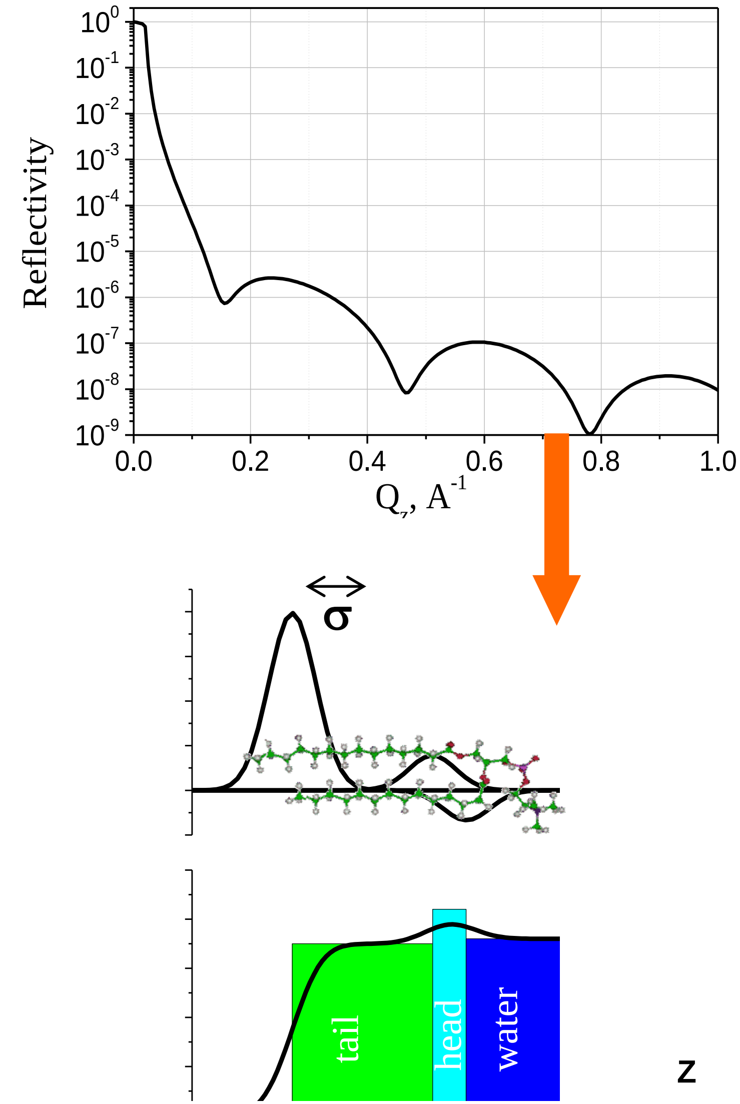

$$I/I_0 = R_F(q_Z)\,|F(q_Z)|^2 \exp(-(q_Z\sigma)^2)$$

where

$q_z = 4\pi \sin(\alpha)/\lambda$

$|F(q_Z)|$ = Fourier transform of $\partial\rho(z)/\partial z$

$$R_F(q_z) = \left(\frac{2\pi}{\lambda}\right)^2 \left|\frac{\sin\alpha - \sqrt{\sin^2\alpha - \sin^2\alpha_C}}{\sin\alpha + \sqrt{\sin^2\alpha - \sin^2\alpha_C}}\right|^2$$

Layering of Nano-Particles at the Air/Water Interface

Sample: **Colloidal suspension of spherical Silica particles (diameter ~320Å) in water a suspension. (Concentrated 40% and dilute 1.8% of weight)**
Aim **: Study of structure organization of nano-particles near air/water interface.**

X-ray reflectivity profiles from the concentrated (a) and dilute sample (b) and from the solvent (c).

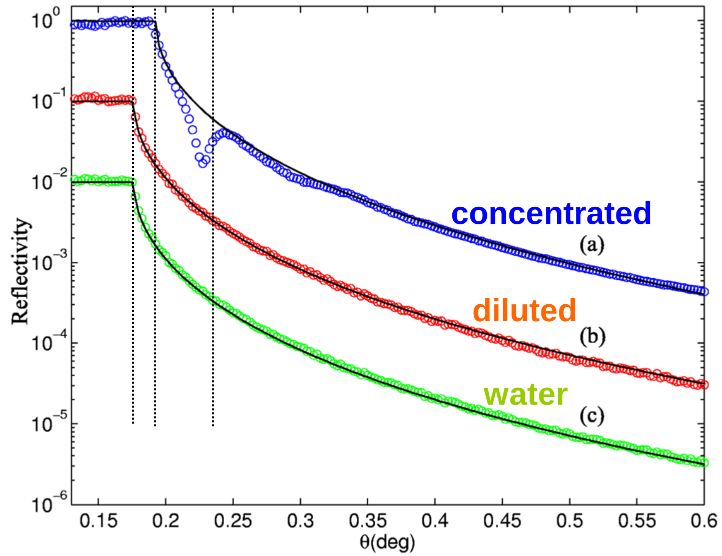

The (b) and (c) curves have been offset by one and two decades respectively. The solid lines are fits of Fresnel's law to the data.

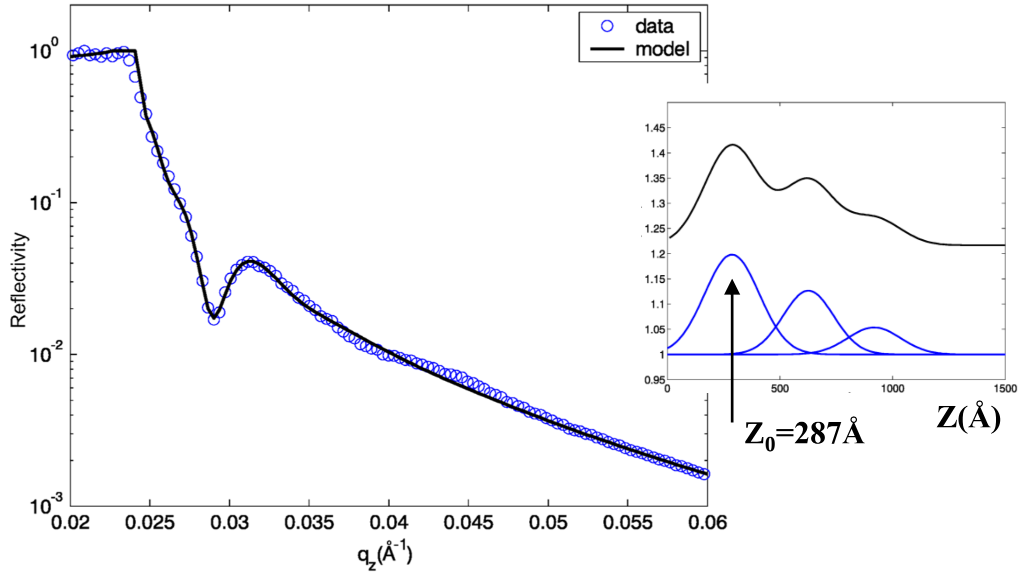

Detailed view of the profile from the concentrated sample and a model fit (solid line) with the SLD profile yielding the best fit shown in the insert)

A. Madsen et al. (2001), PRE 64, 061406

Lipid monolayers on water, sol and gel surface

I) Gelation of clays

Montmorillonite

Used as additive in many industrial processes

The Mineral

- *Phyllosilicate*
- *Disc shaped nano particles*
- *Surface area ~400 m^2/g*
- *Charge deficiency of 0.7 / unit cell*
- *Charging: surface ⊖ , edges ⊕*
- *With water: gives clear and colourless dispersions and gels*

The Gel

- *Thixotropic, highly viscous*
- *Ionic bonds, not affected by temperature*
- *Gel Formation at concentrations < 1% in water*

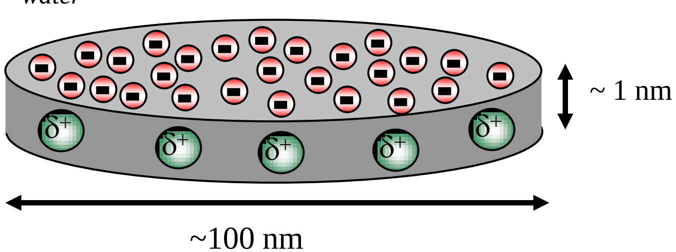

Dry: Aggregated Particles

Sol

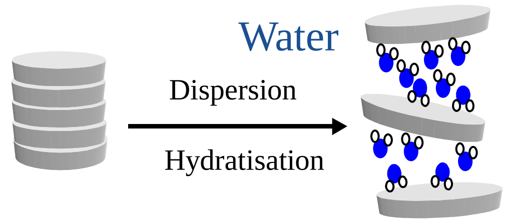

After some hours:
Gel formation – House of cards

II) Phosholipids

DSPC

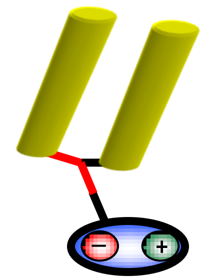

DPPA

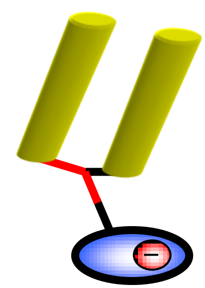

Struth B., et.al. Phys. Rev. Let., 88, 25502, (2002)

Lipid monolayers on water, sol and gel surface

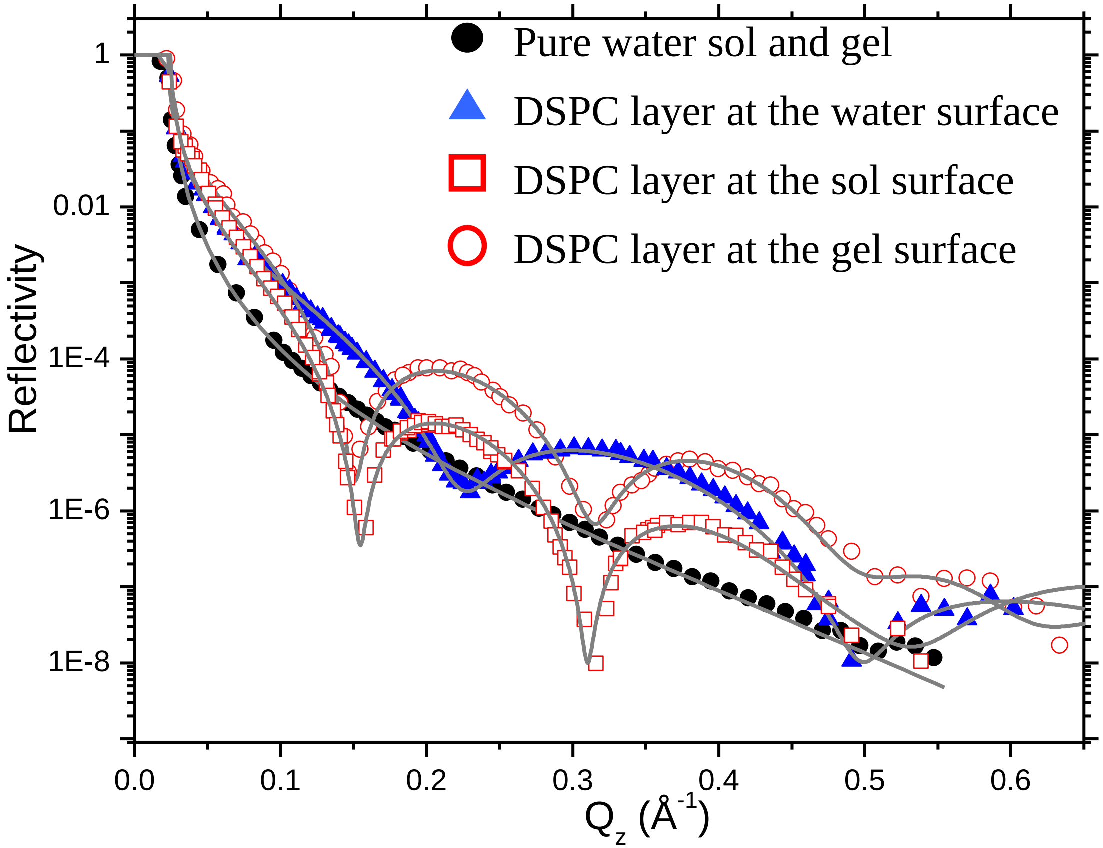

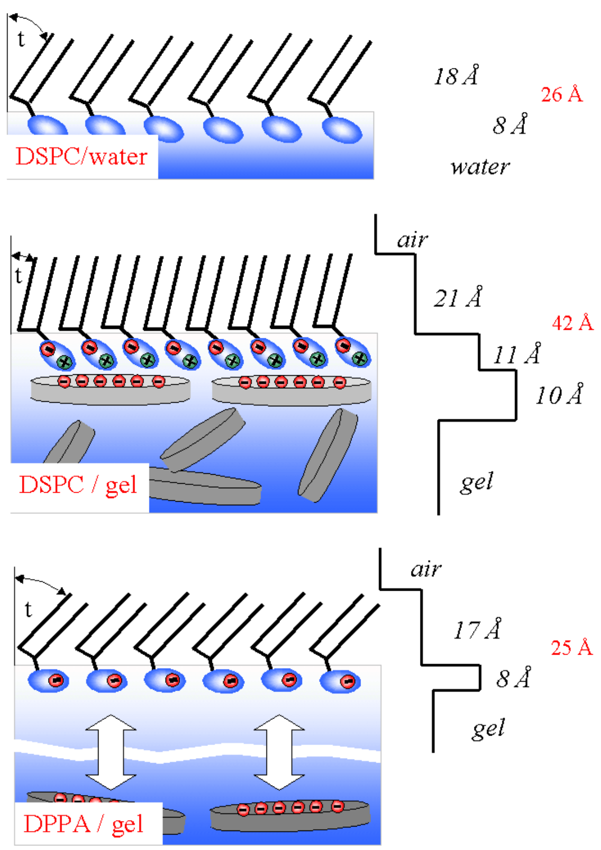

- *Identical roughness of free water, sol and gel surfaces*
- *Lipids form stable monolayers on water, sol and gel*
- *Attractive electrostatic interactions between the anionic mineral particles and the zwitterionic lipid headgroup*
- *These interactions influence the lateral lattice of the monolayer*

Struth B., et.al. Phys. Rev. Let., 88, 25502, (2002)

Reflectivity measured and model of electron density profile before and after injection of C-cadherin in the subphase

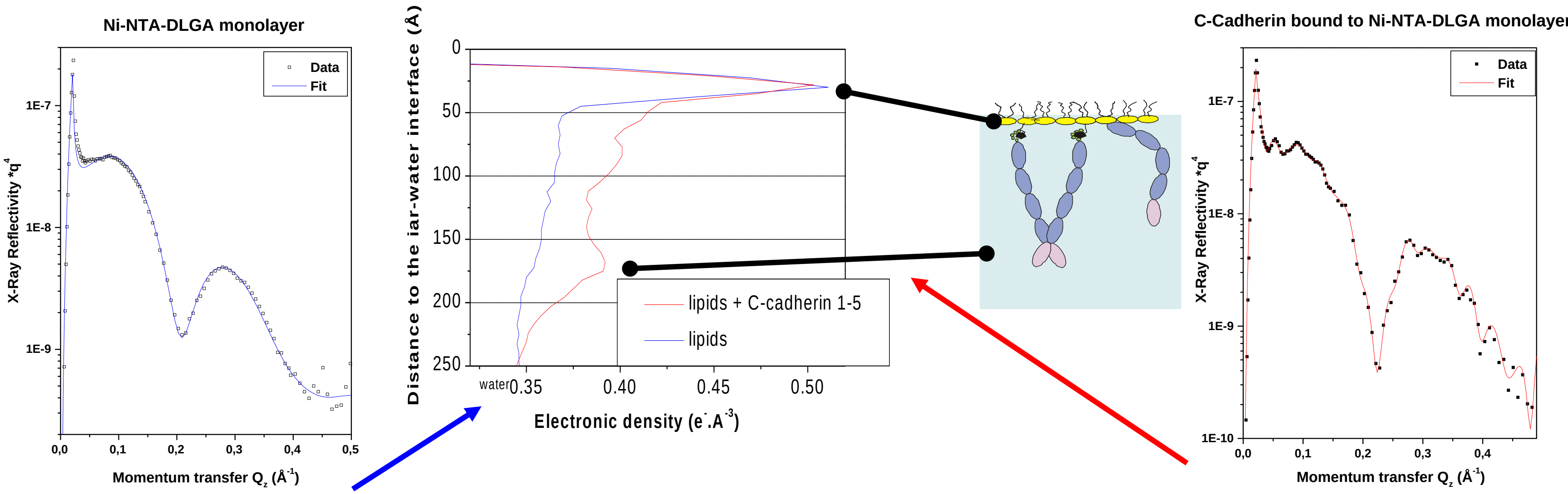

• Cadherins extend over 230Å. That is shorter than cadherin length : cadherin may **be curved**

• High density at large distance : **parallel interactions ?**

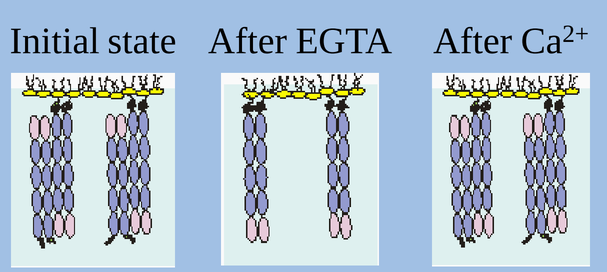

1) After injecting proteins in the subphase, a homogenous layer is obtained in 4 hours
2) The decrease of bound proteins after adding chelates divalent ions EGTA is interpreted as a partial dissociation of adhesive dimers
3) Subsequent addition of calcium restores the dimers

Ca influence

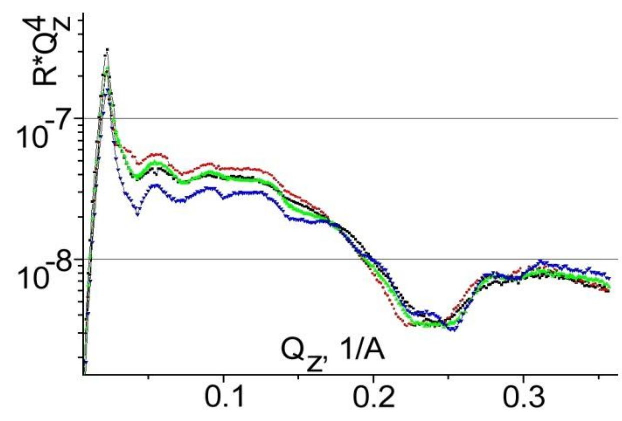

L. Martel, et. al., J. Phys. IV France, ***v.12****, 365 (2002)*

Grazing Incidence Diffuse Scattering

Liquid-Vapour Interfaces at Short Length Scales

Liquid-vapour interfaces, are common in both natural and artificial environments

Liquid-vapour interfaces were first described, in 1893 by van der Waals, as regions of continuous variation of density caused by density fluctuations within the bulk phases In contrast, the more recent capillary-wave model (1965, F.P.Buff, R.A.Lovett, R.H.Stillinger)) assumes a step-like density profile across the liquid-vapour interface, whose width is the result of the propagation of thermally excited capillary waves.

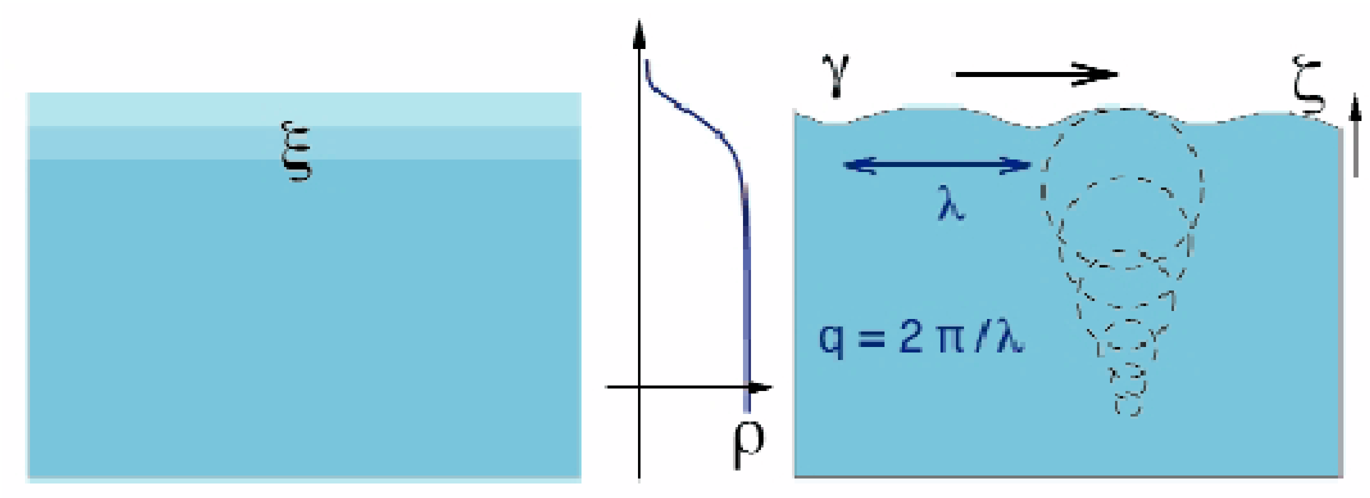

The model has been validated for length scales of tens of micrometres and larger, but the structure of liquid surfaces on submicrometre length scales, where the capillary theory is expected to break down, remains poorly understood. One reason is that, in contrast to solid surfaces, the absence of relevant experimental information even for the simplest liquid-vapour interfaces precludes the assessment of any of the existing theories which considerably diverge in their conclusions

C. Fradin et al., Nature, ***403****, 871-874, (2000)*

Diffuse scattering on liquid surface

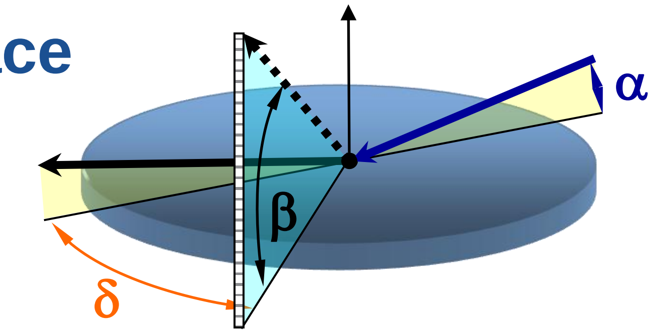

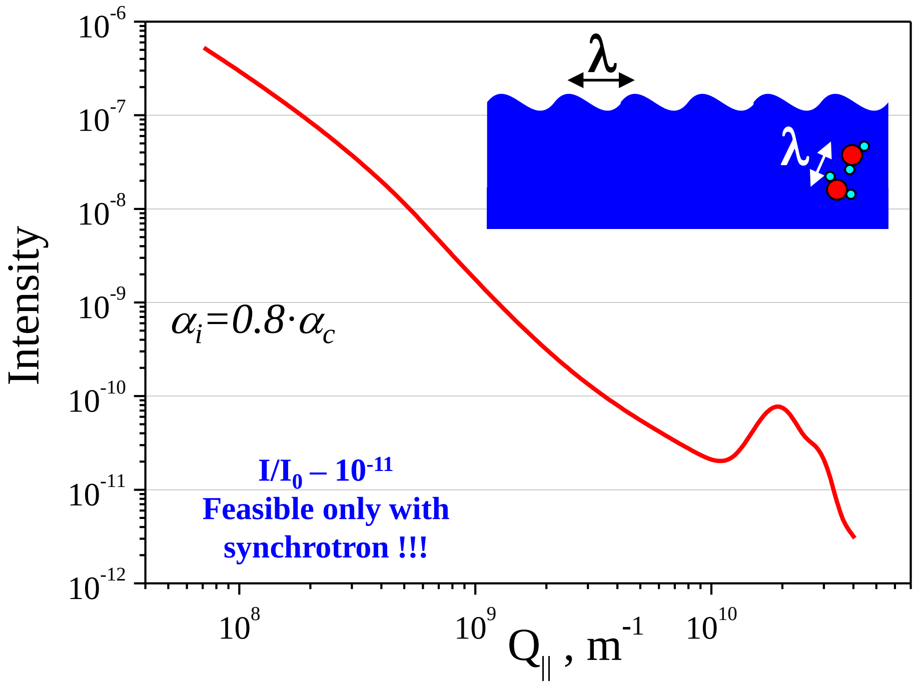

Capillary waves -> height correlation spectrum determided by the surface energy (γ) assocoated with the deformation modes (κ) *[Helfrich, Z. Naturforsch., 28c , 693, (1973)]*

$$\left\langle z(q_\parallel)\,z(-q_\parallel)\right\rangle = \frac{1}{A}\,\frac{k_B T}{\Delta\rho g + \gamma q_\parallel^2 + \kappa q_\parallel^4}$$

$$\left(\frac{d\sigma}{d\Omega}\right) \approx A\,\frac{k_0^4\theta_c^4}{16\pi^2}\left|t^{in}\right|^2\left|t^{sc}\right|^2\left[\frac{k_B T}{\gamma\, q_\parallel^2}\left(\frac{q_\parallel}{q_{\max}}\right)^{\eta} + \frac{k_B T \kappa_T}{2\,\mathrm{Im}\left(q_z^t\right)}\right]$$

C. Fradin et al., Nature, ***403****, 871-874, (2000)*

conformal roughness

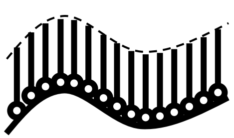

$$\frac{d\sigma}{d\Omega} \approx A r_e^2\left|t_{0,1}^{in}\right|^2\left|t_{0,1}^{sc}\right|^2\left|\tilde{\rho}(q_z)\right| e^{-q_z^2<z^2>}\int d\,\mathrm{r}_\parallel\left(e^{q_z^2<z(0)z(\mathrm{r}_\parallel)>}-1\right)e^{i\,\mathrm{q}_\parallel \mathrm{r}_\parallel}$$

Scale-dependent surface tension

Using grazing-incidence X-ray scattering, the first complete determination of the free surface structure and of the wavevector-dependent surface energy for water and organic liquids was obtained.
Observed ⇨ A large decrease of the surface energy of sub-micrometer waves, which cannot be explained by the phenomenological capillary theories, and which is decisive in the long-standing dispute on structure of liquid interfaces.

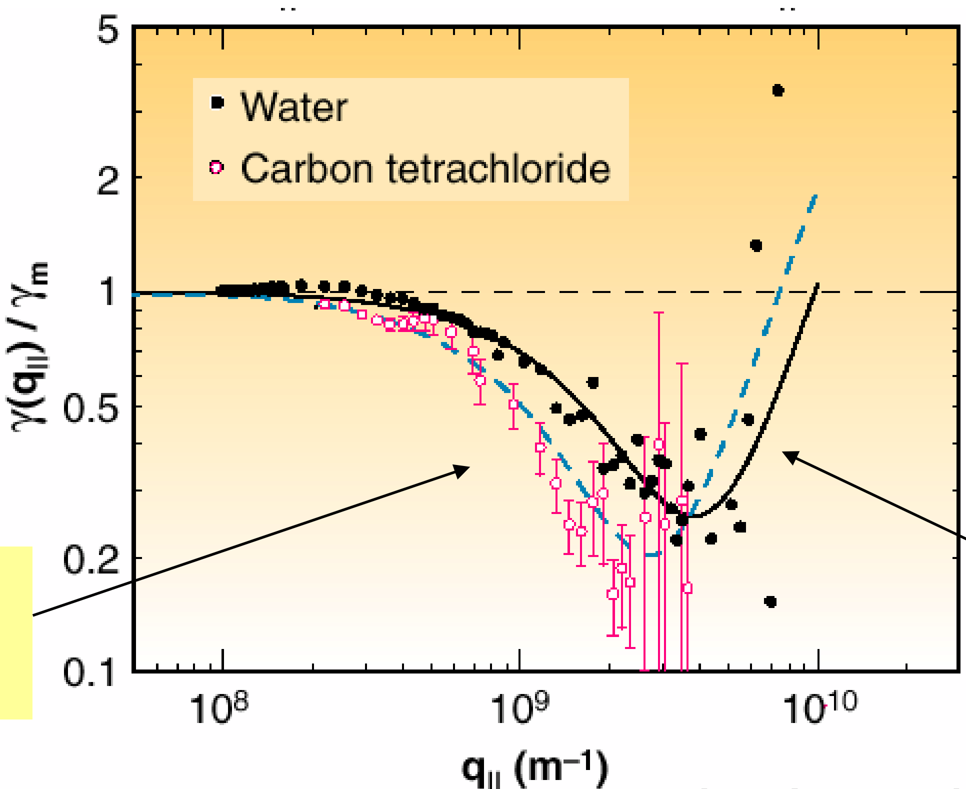

Long-ranged power-law decay of the dispersion forces between the fluid particles

Distortion of density profile when surface is bent

*K.R. Mecke and S. Dietrich, Phys. Rev. E., v.**59**, 6766 (1999)*

Grazing Incidence Diffraction

(Two dimensional crystals)

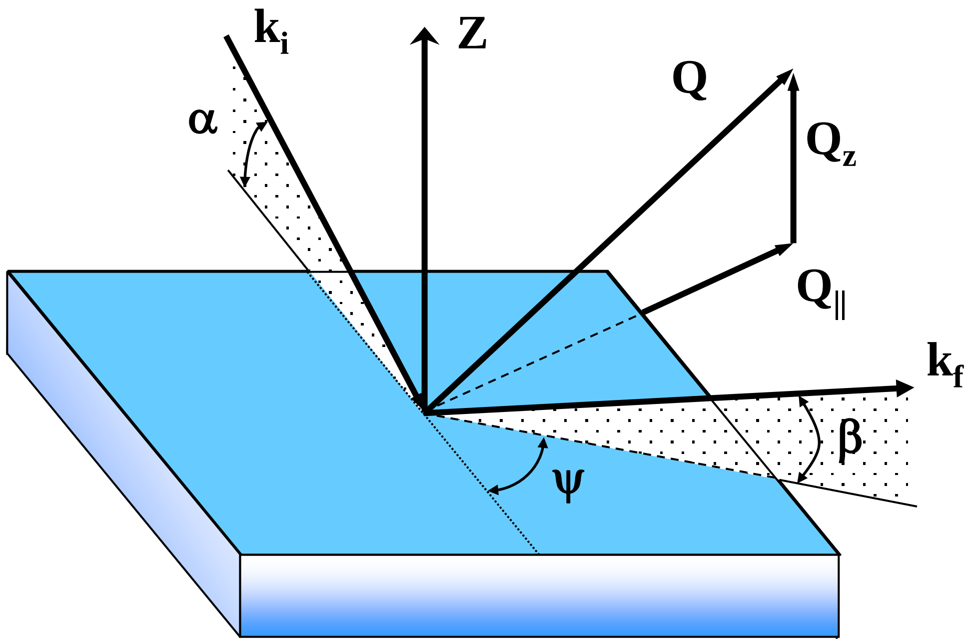

Diffraction from 2D array of rodlike molecules

Real space → Reciprocal space

Rod like molecule

2D lattice

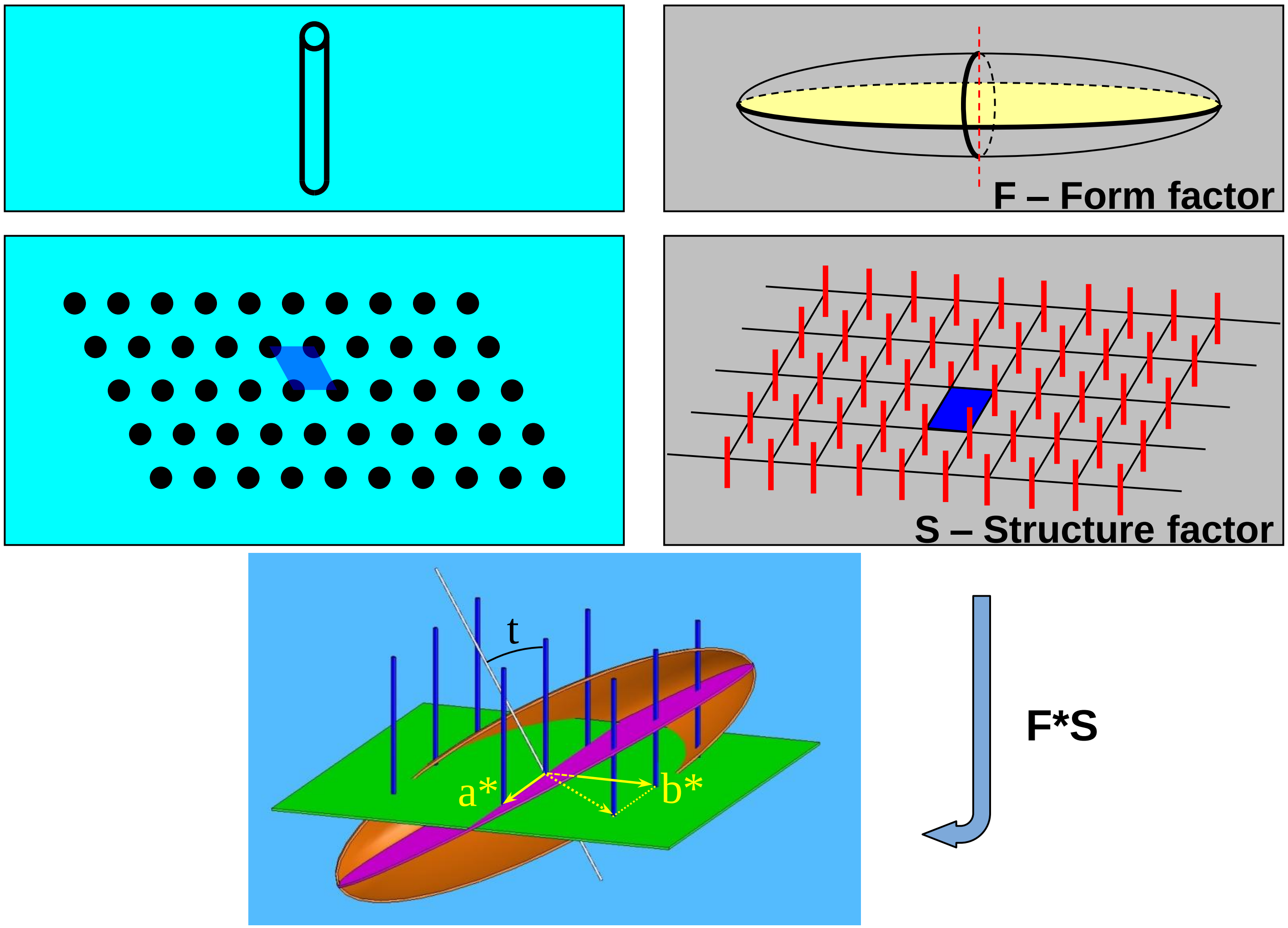

GI Diffraction from 2D array of rodlike molecules

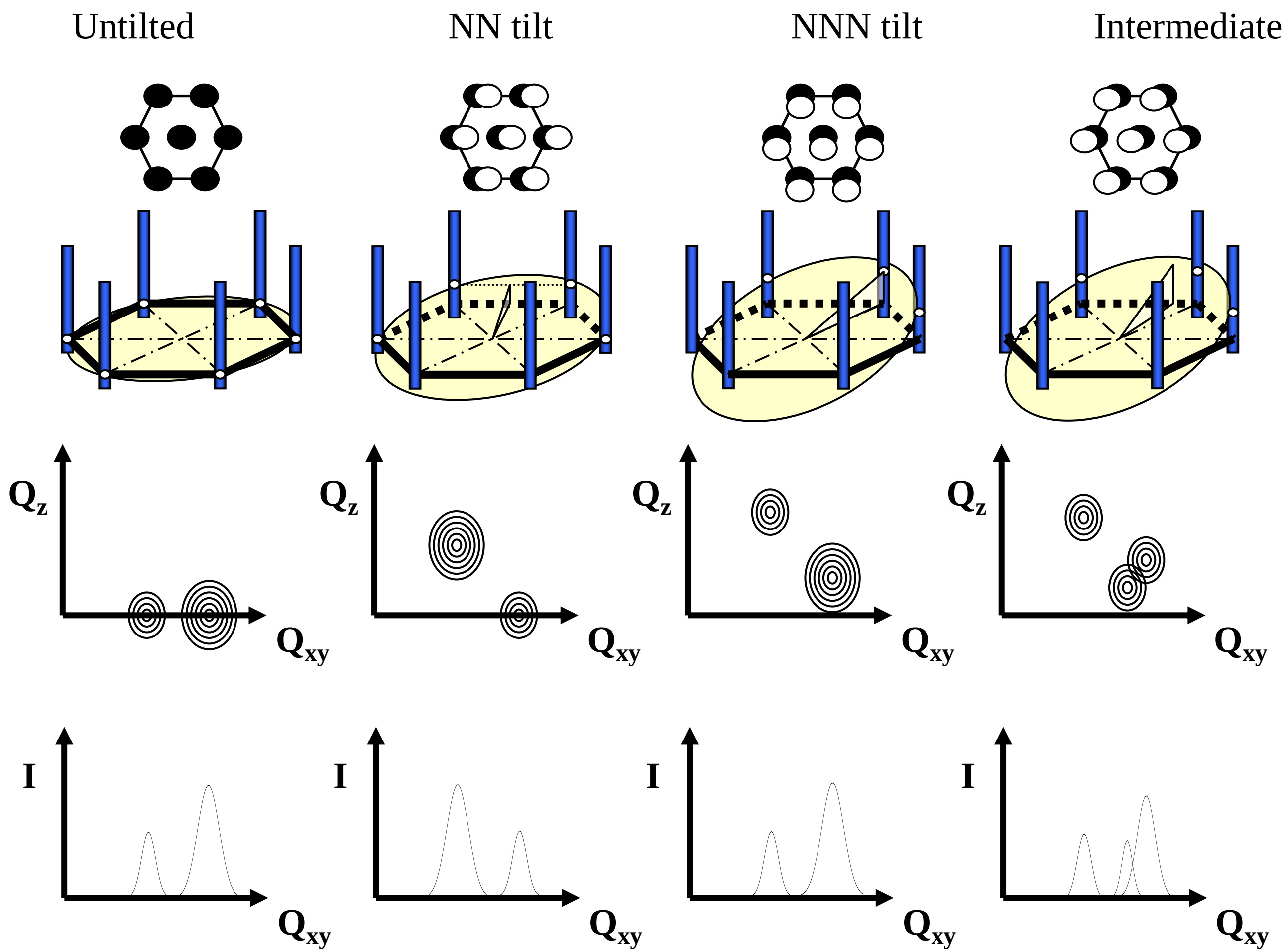

Output:
Lattice parameters, tilt angle & azimuth, correlation length, molecular length and structure.

Kaganer et al., Reviews of Modern Physics, ***71*** *(1999) 779*

Typical GID map obtained on monomolecular film of lipids DPPC at 30 mN/m on the air/water interface

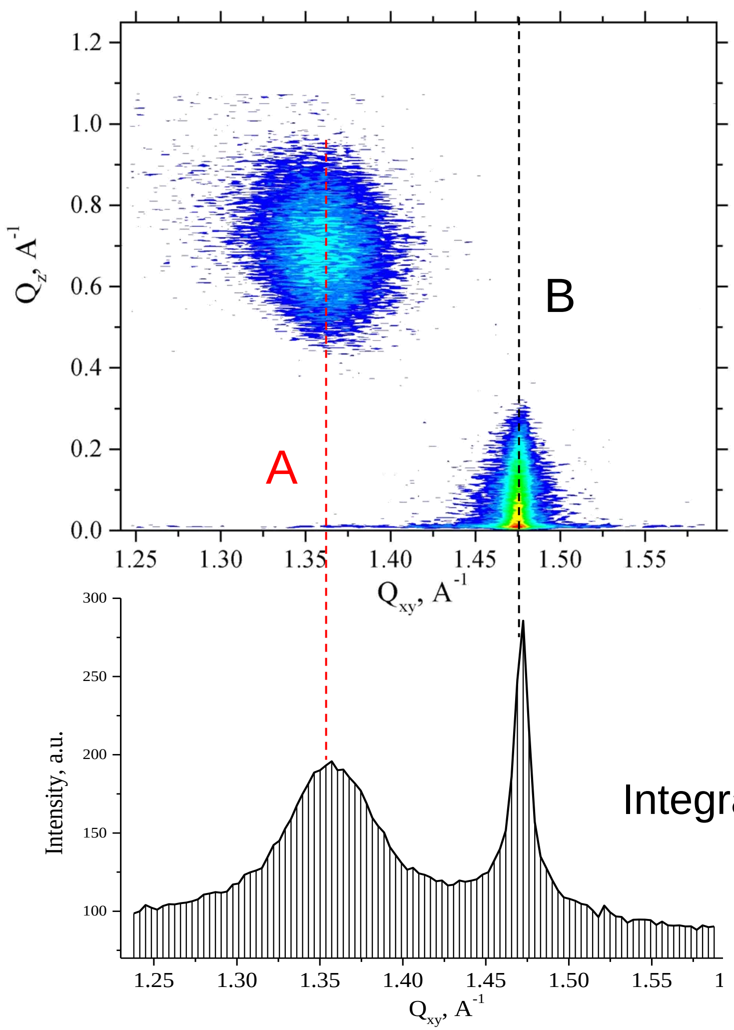

Integrated map

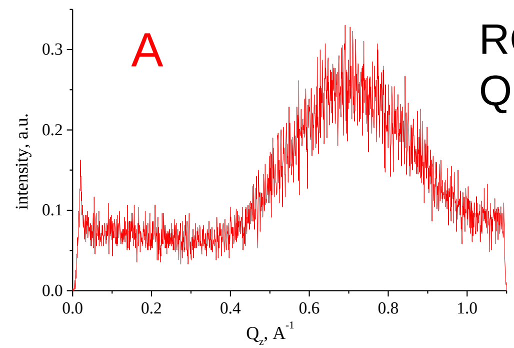

ROD (10)(01)
$Q_{||}$=1.357 A^{-1}

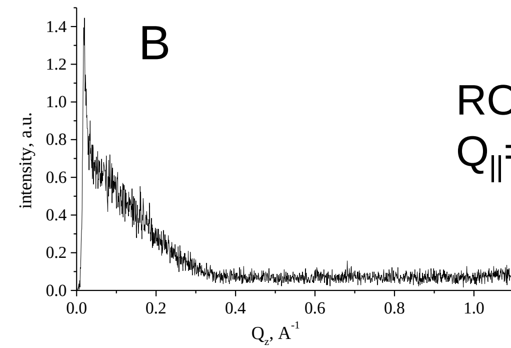

ROD (11)
$Q_{||}$=1.472 A^{-1}

Molecular form factor

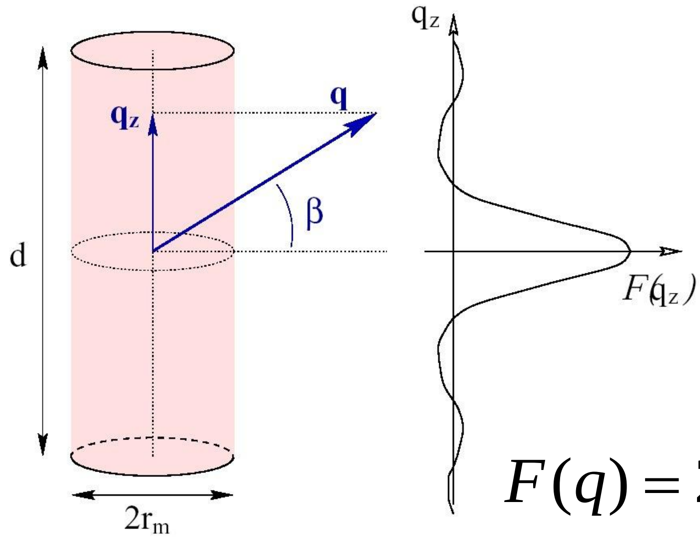

$$F(q) = \int_0^{r_m} \int_{-\pi}^{\pi} \int_{-d/2}^{d/2} \rho_e e^{iqr} r dr d\alpha dz$$

$$F(q) = 2\pi d \rho_e \frac{\sin\left(qd\sin(\beta)/2\right)}{qd\sin(\beta)/2} \int_0^{r_m} r J_0(qr\cos\beta) dr$$

$$if \quad J_0(qr\cos\beta) \approx 1 \quad \left(@ \quad qr_m \cos(\beta) << 1\right) \quad and \quad Z_m = \pi r_m^2 d \rho_e$$

$$F(q) = Z_m \frac{\sin\left(qd\sin(\beta)/2\right)}{qd\sin(\beta)/2}$$

$$I(q_z) \approx \left(\frac{\sin\left((q_z - q_{zM})t/2\right)}{q_z t/2} \right)^2$$

t – film thickness

What to do with measured Bragg rods $Q_1(\parallel,\perp)$ $Q_2(\parallel,\perp)$ $Q_3(\parallel,\perp)$?

(simple way to solve 2D structure)

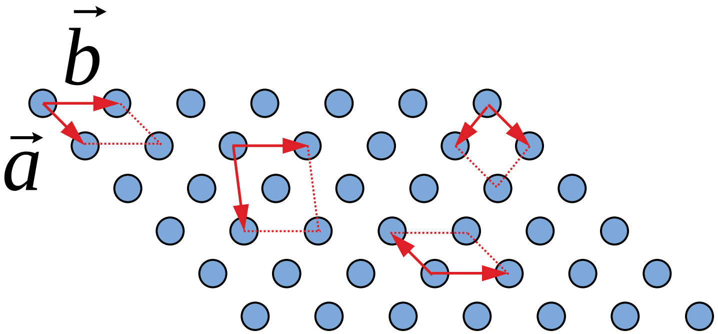

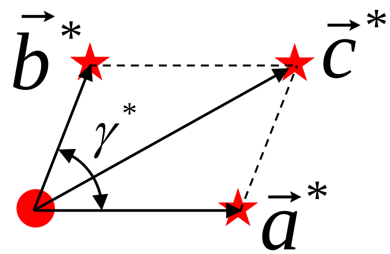

$$\vec{c} = \vec{a} + \vec{b}$$

$$\gamma^* = \pi - \gamma$$

$$c_\parallel^{*2} = a_\parallel^{*2} + b_\parallel^{*2} - 2a_\parallel^* b_\parallel^* \cos\gamma$$

$$a = \frac{2\pi}{a_\parallel^* \sin\gamma}$$

$$b = \frac{2\pi}{b_\parallel^* \sin\gamma}$$

$$\vec{m} = (\vec{a}^* - \vec{b}^*) \times (\vec{c}^* - \vec{b}^*)$$

$$\vec{m} \cdot \vec{n} = |\vec{m}| \cdot |\vec{n}| \cos\theta$$

$$\vec{m}_\parallel \cdot \vec{a} = |\vec{m}_\parallel| \cdot |\vec{a}| \cos\psi$$

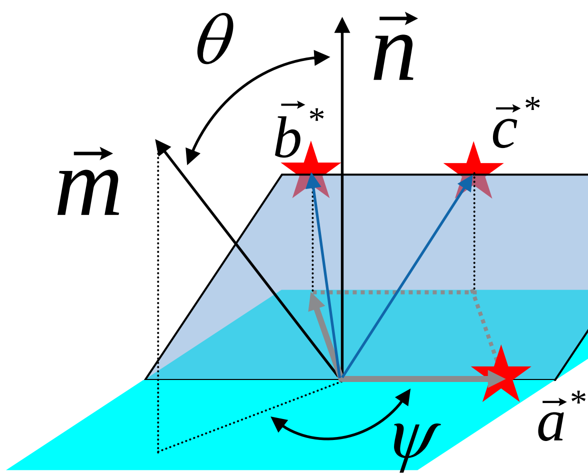

Behenic acid (C_{22}) phase diagram

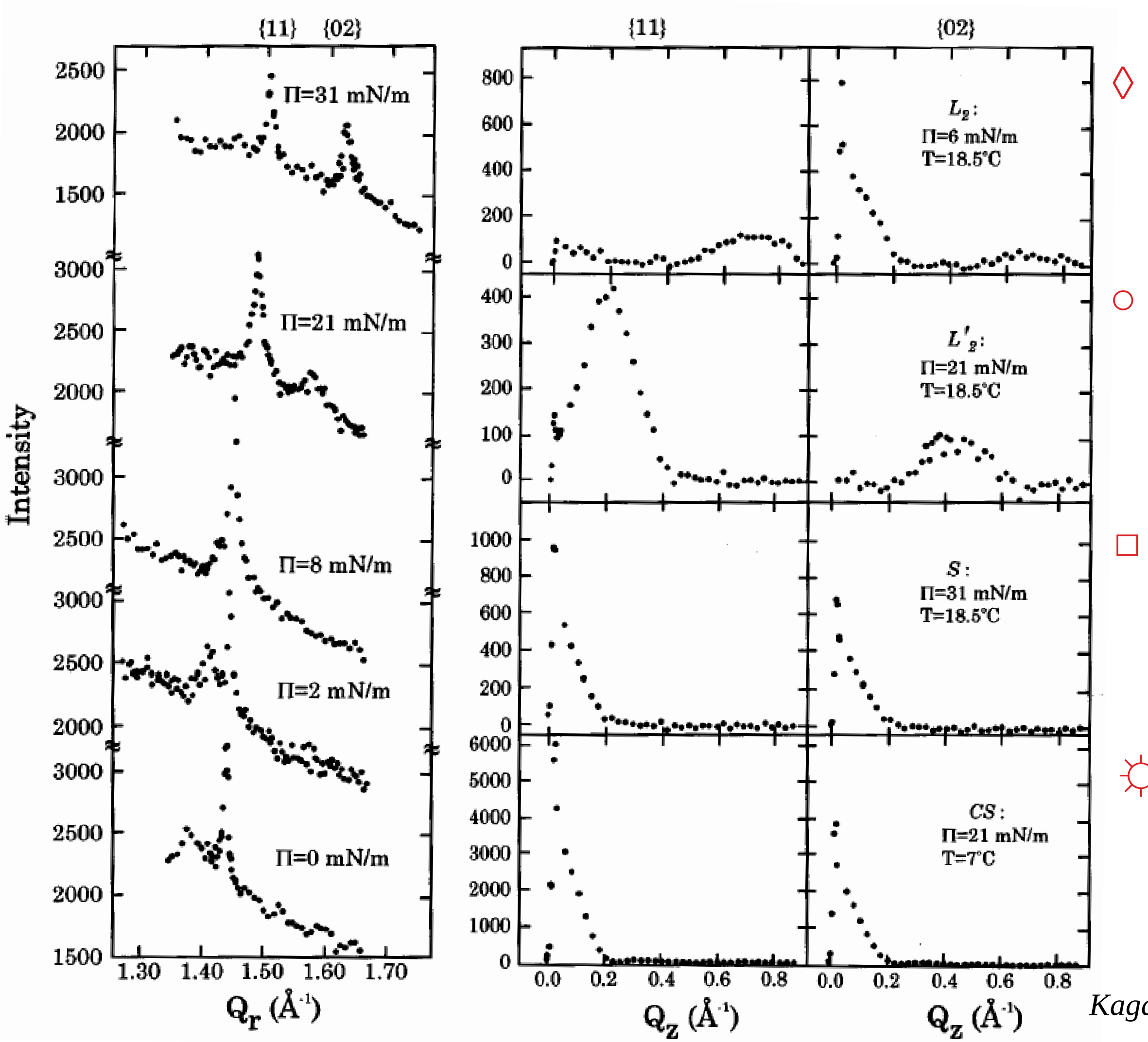

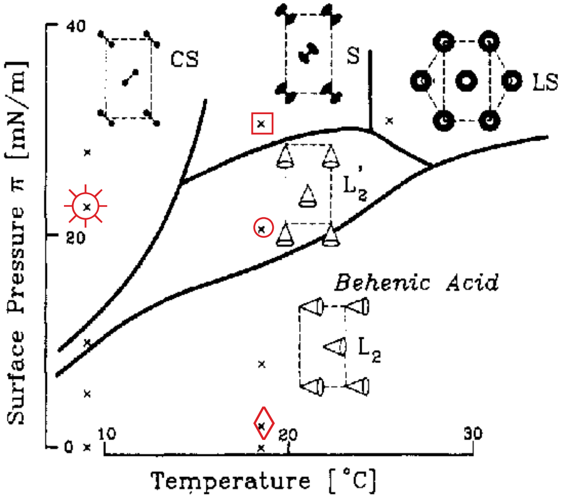

*Kaganer et al., Reviews of Modern Physics, **71** (1999) 779*

Kenn, et al., The Journal of Physical Chemistry, Vol. 95, No. 5, 1991

GID: 2D Lattice Compressibility

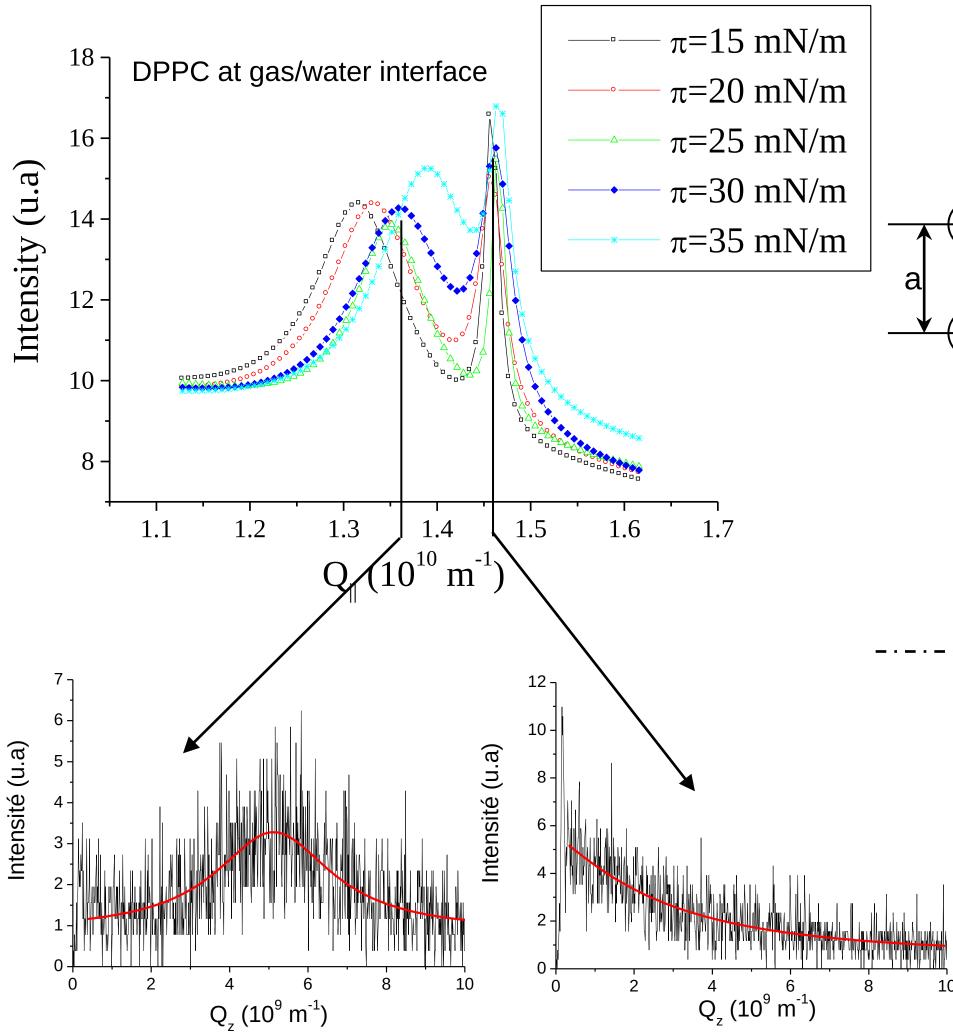

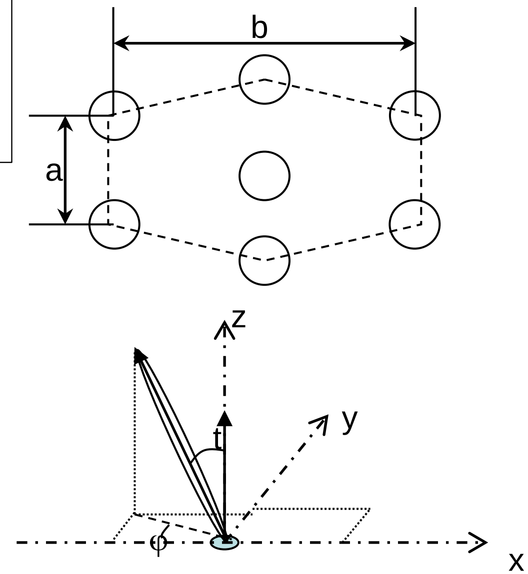

Isothermal compressibility χ

$$\chi = -\frac{1}{A} \times \left(\frac{\partial A}{\partial \pi}\right)_T$$

Landau theory

⇩

Bending rigidity κ

⇩

$$\kappa = \frac{h^2}{12 \times k_b T \times \chi}$$

h – film thickness

	Rigidity κ ($k_B T$) $\pi < \pi_{cp}$ of PGLa	Rigidity κ ($k_B T$) $\pi > \pi_{cp}$ of PGLa
DPPC	15	17
DPPG	30	45

Two dimensional protein crystallography

Soluble and membrane proteins do not form 3D crystals
But can be assembled in 2D crystals using surface-bound affinity ligands or surface-bound charged lipids

Electrostatic interaction
Annexin V + DOPC
DOPC:DOPS (4:1)

Molecular recognition
Streptavidin + biotine-LC-DPPE
DPPE: biotine-LC-DPPE (4:1)

Binding of histidin-tag with Ni chelated lipids
HupR + Ni-NTA-DOGA
DOPC : Ni-NTA-DOGA 3:1

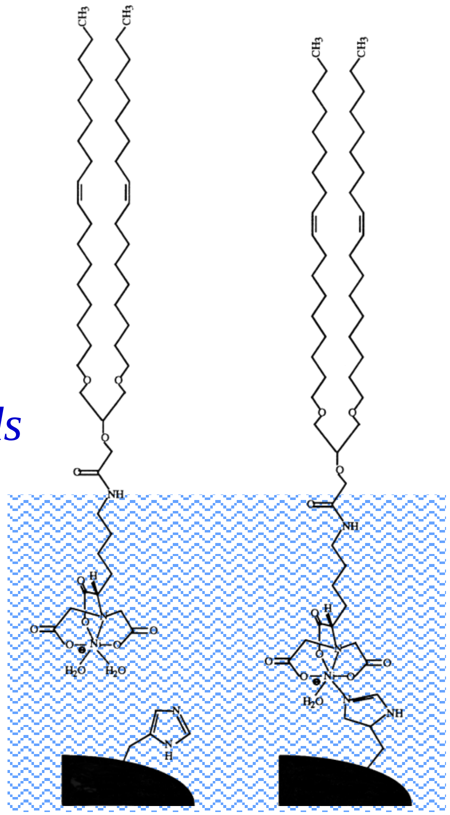

Electron micrograph of HupR crystals

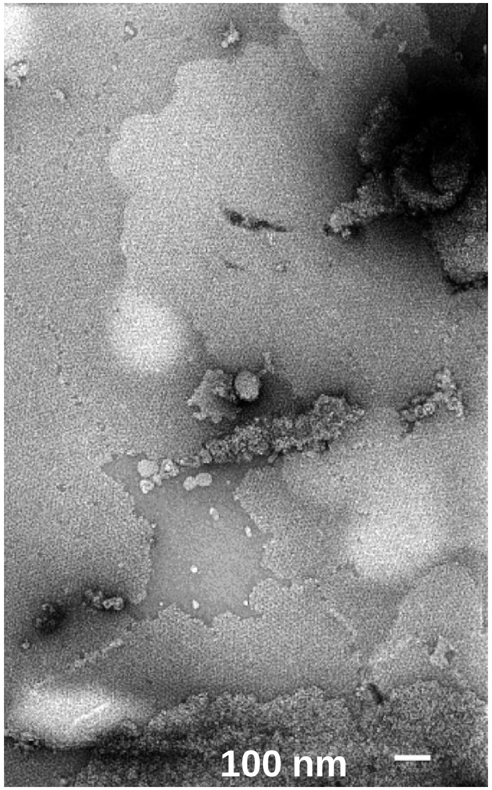

<u>Three steps of 2D crystal formation</u>

1. Molecular recognition
2. Diffusion and concentration
3. Self assemble of the protein

*S. Courty et al., Langmuir, **v. 18**, 9502 (2002)*

2D protein crystals: Towards atomic resolution

Streptavidin

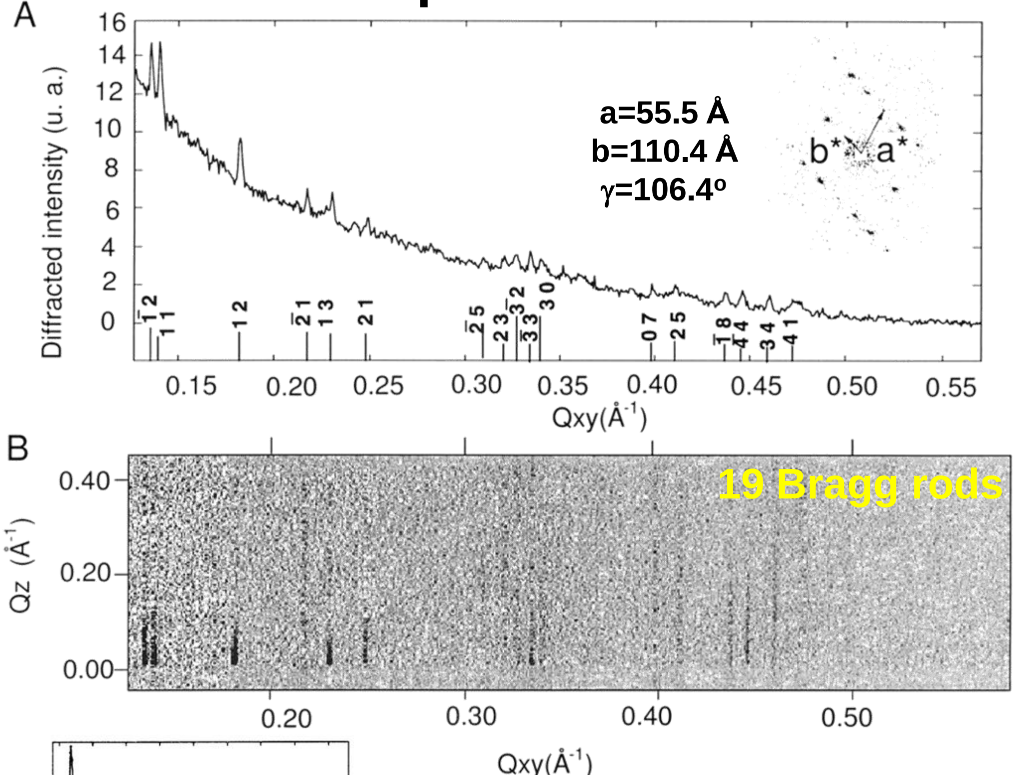

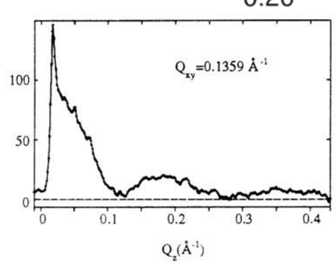

⇦ Bragg rod (-12)

P.-F. Lenne et al.,Biophysical Journal, v. 79, 496 (2000)

Behenic acid

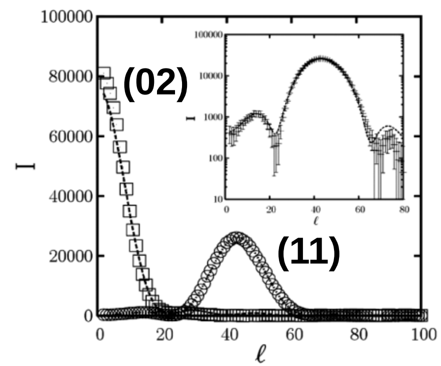

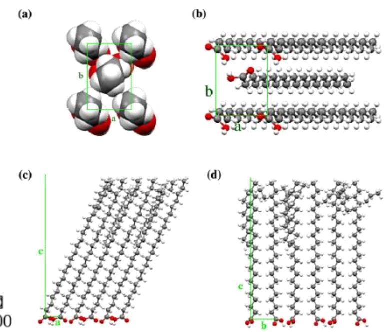

Reflections intensity ratio

→ **orientation of the backbone planes**

Bragg rod profiles

→ **conformation defects in the hydrocarbon chain**

J. Pignat et al., Thin Solid Films, 515, 5690, (2007)

Effect of OH group position on the 2D structure of Langmuir monolayers of hydroxystearic acids

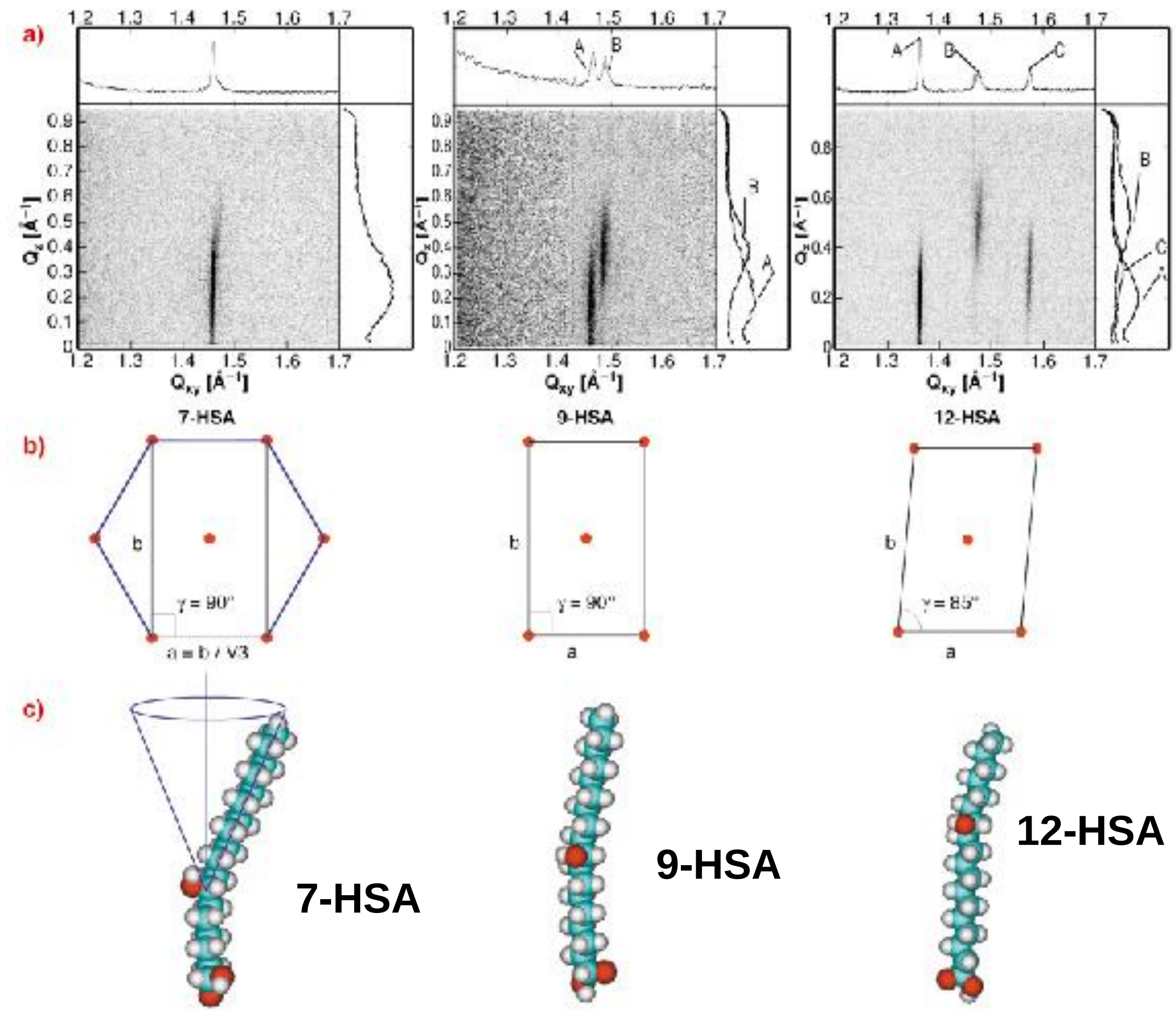

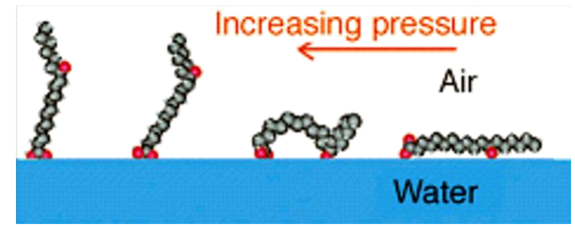

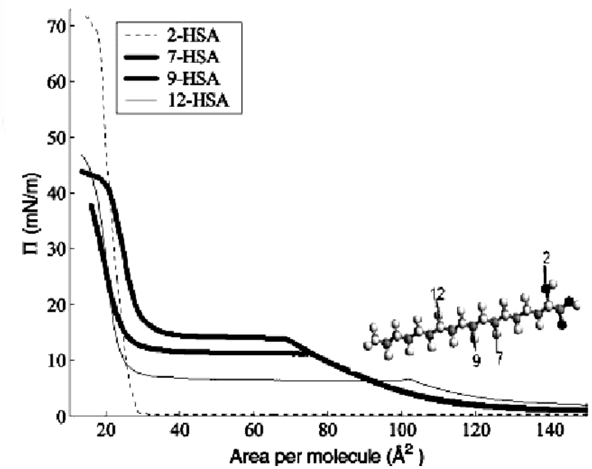

GID patterns for molecules:
7HSA (@16 mN/m)
9HSA (@12 mN/m)
12HSA (@7 mN/m)
T=20ºC.

Rotor phase is proposed for molecular conformation of 7HSA,

L. Cristofolini et al., Langmuir, v. 21, 11213 (2005)

Template growth of nanocrystalline PbS, CdS and ZnS on a polydiacetylene (PDA) Langmuir film

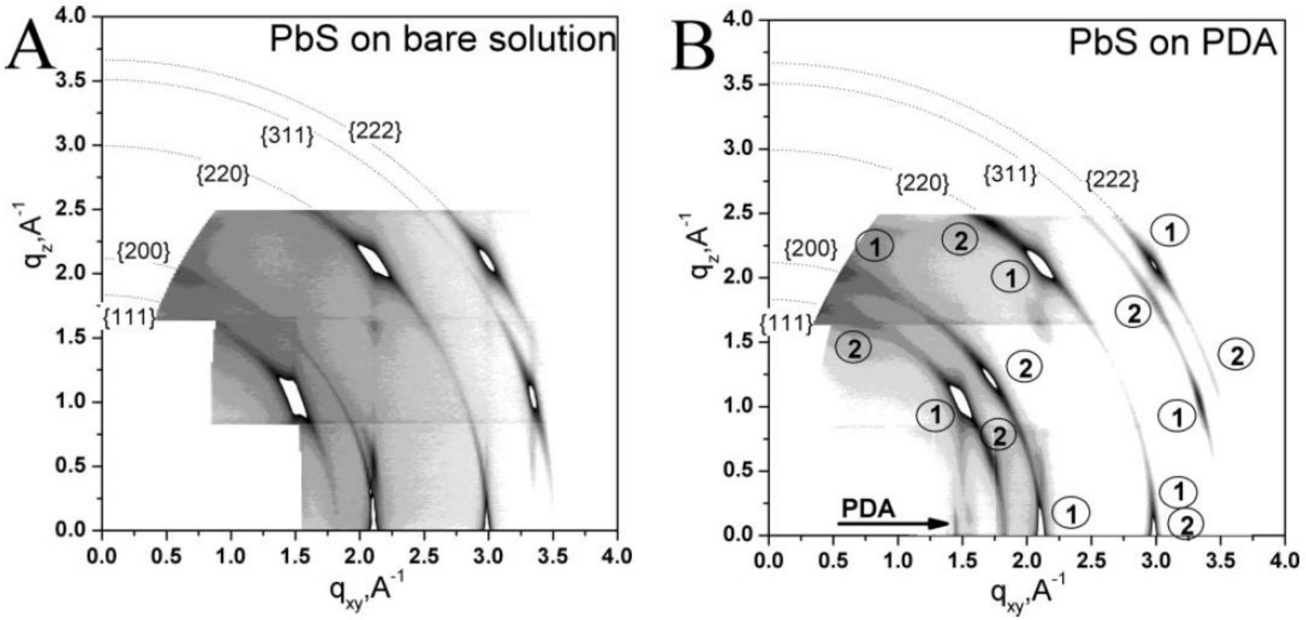

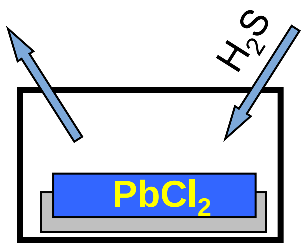

π=25 mN/m
C=0.2 mM
UV

GID reciprocal maps of PbS nanocrystals at the air/solution interface. (A) in the absence of PDA and (B) in the presence of a PDA film. In (A) a single (100) orientation is observed. The notations (1) and (2) in (B) denote reflections corresponding to the (100) and (111) orientations, respectively. The reflection marked with an arrow in (B) corresponds to the PDA template

Y. Lifshitz et al., Adv. Funct. Mater., v.16, 2398–2404, (2006)

Grazing Incidence Small Angle Scattering

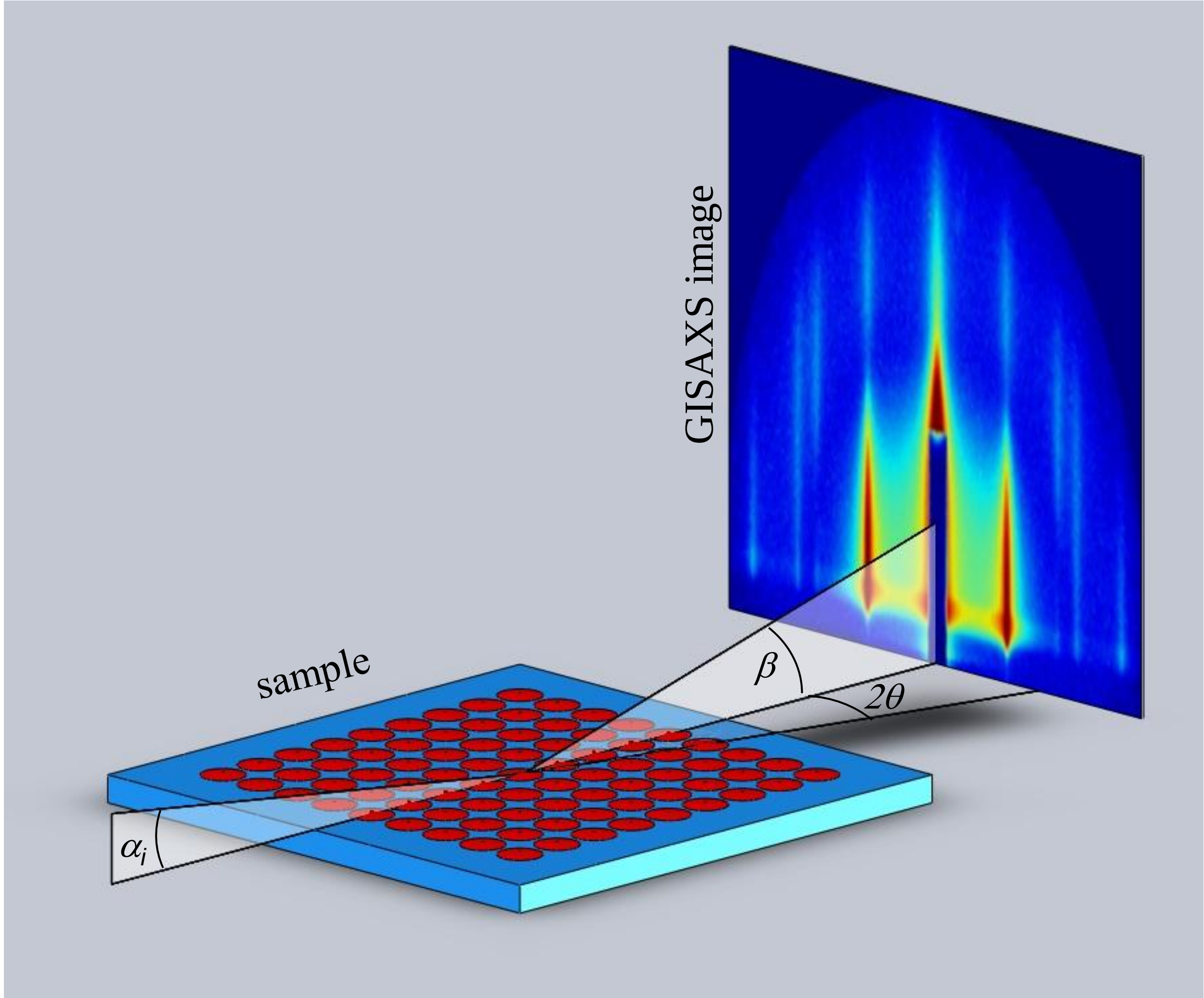

Direct Evidence for Highly Organized Networks of Circular Surface Micelles of Surfactant at the Air-Water Interface

$C_8F_{17}C_{16}H_{33}$ hemimicelles

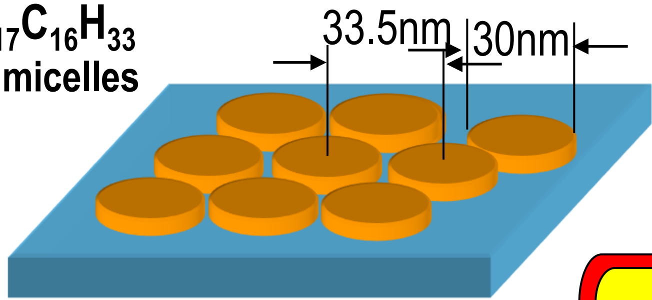

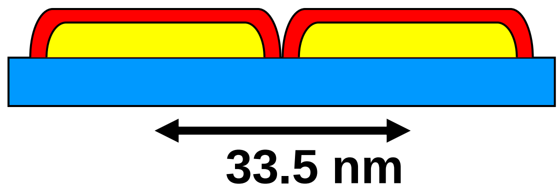

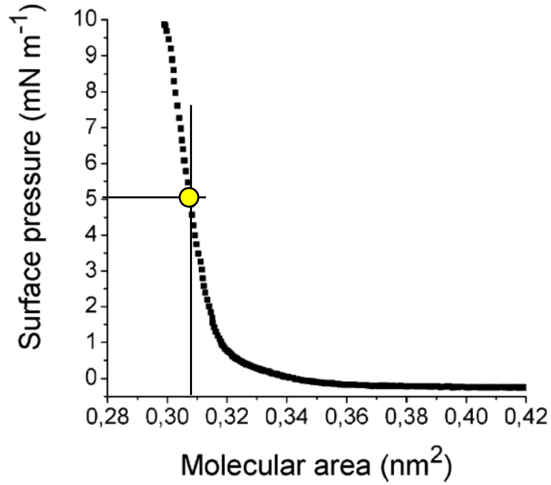

parameters of the setup:
beam 0.25×0.1 mm^2 (H×V)
λ=1.55Å (E=8keV)
α=2 mrad ($α_c$=2.5 mrad)
linear PSD (vertical) Q_z^{max}=5nm^{-1}
in-plane resolution 1 mrad

π=5 mN/m
T=20°C

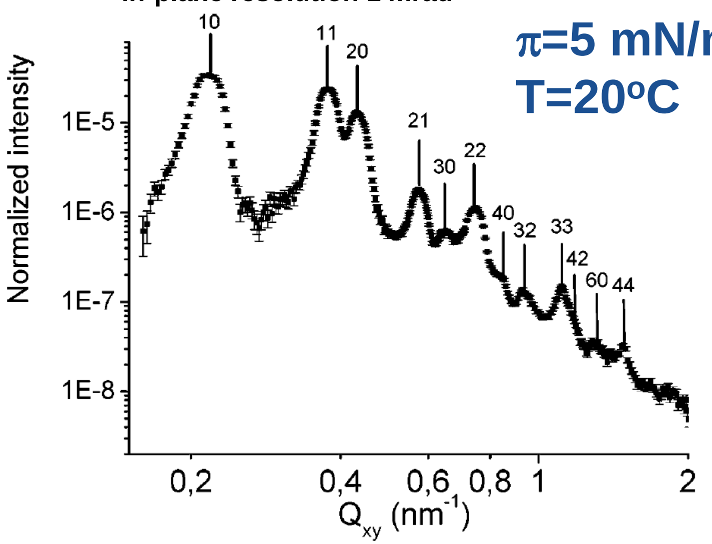

Table 1. Peak Positions (Q_{xy}) and Widths (W) Deduced from a Lorentzian Fit of the Diffraction Peaks[a]

Q (nm^{-1})	W (nm^{-1})	indexation (hexagonal lattice)
0.2159	0.0249	(1 0)
0.3772	0.0303	(1 1)
0.4333	0.0307	(2 0)
0.575	0.033	(2 1)
0.6509	0.0299	(3 0)
0.747	0.0467	(2 2)
0.8478	0.0222	(4 0)
0.939	0.044	(3 2)
1.113	0.0524	(3 3)
1.172	0.0362	(4 2)
1.293	0.068	(6 0)
1.482	0.0438	(4 4)

[a] Last column is the indexation of the peaks in a hexagonal lattice with a parameter of 33.5 nm.

*Fontaine et al., J. Am. Chem. Soc. **127**, p.512 (2005)*

Reversible buckling in monolayer of gold nanoparticles on water surface

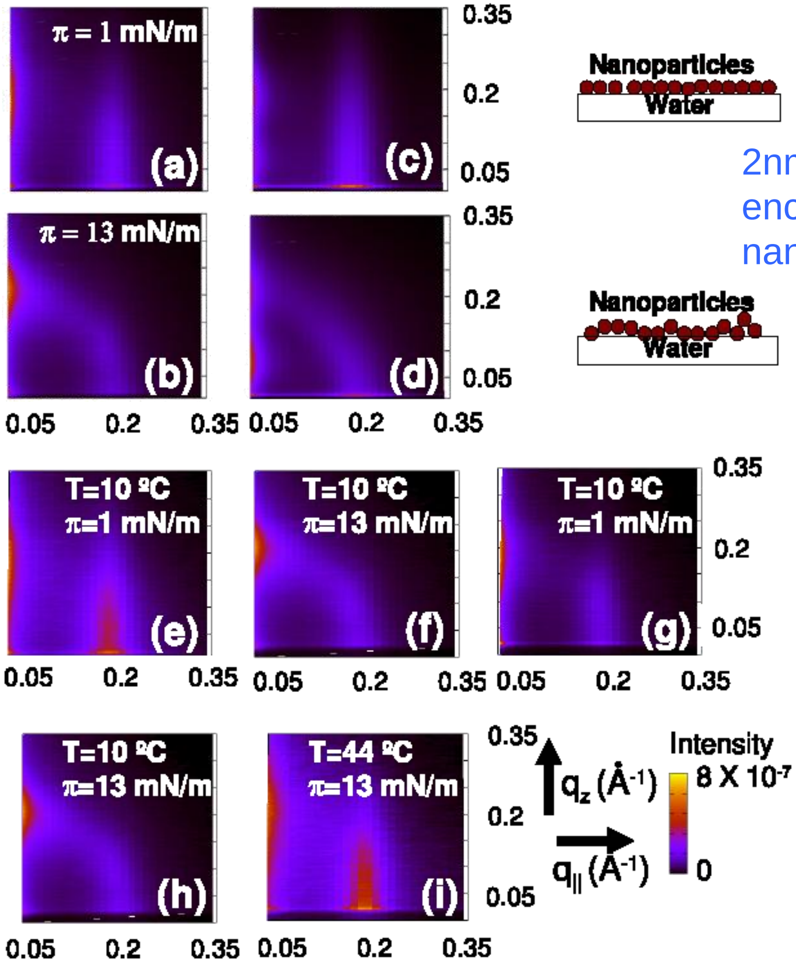

2nm dodecanethiol-encapsulated gold nanoparticles

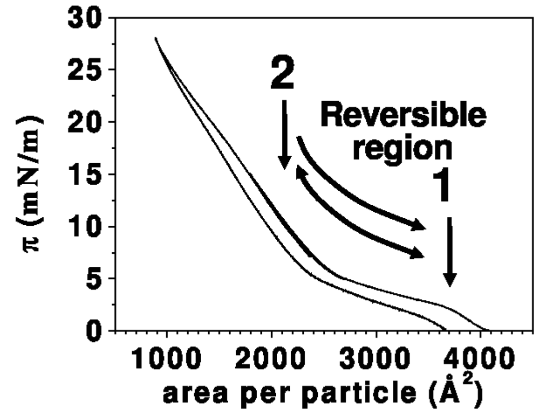

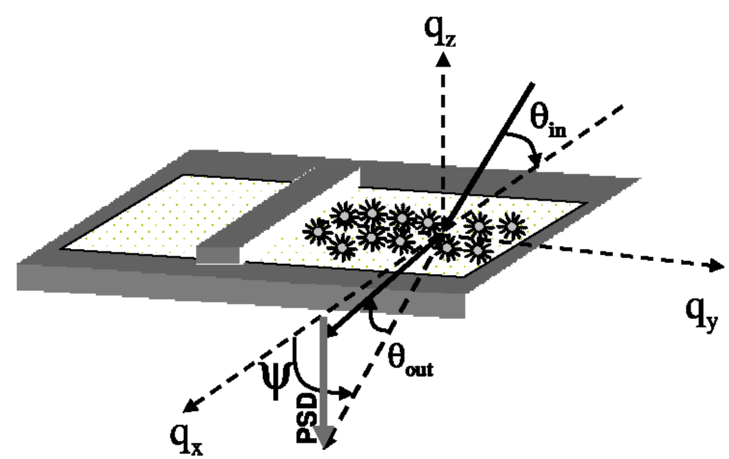

M. K. Bera et al., EPL, v. 78, 56003, (2007)

Buried Interfaces

The liquid-liquid and liquid-solid interfaces play an important role in many physical, chemical and biological processes of everyday life. Its characterization would enhance our understanding of fundamental processes occurring in nature.

- Molecular ordering of the liquids near and within LL interfaces
- Surfactants and ions ordering at the LL interface
- Bio-mimetic systems (model membranes at LL and LS interfaces)
- Bio-mineralization
- Emulsion (fundamental aspects and applications: food industry, paints, hydrometallurgy ...)
- Studies of reactions, interfacial synthesis
- Growth and ordering of nano particles
- Electrochemical processes
- Photochemistry at LL Interfaces
- ….

X-ray scattering at Liquid/Liquid Interfaces: Attenuation length

- **Penetration**
- **Background**
- **Meniscus**

Attenuation length

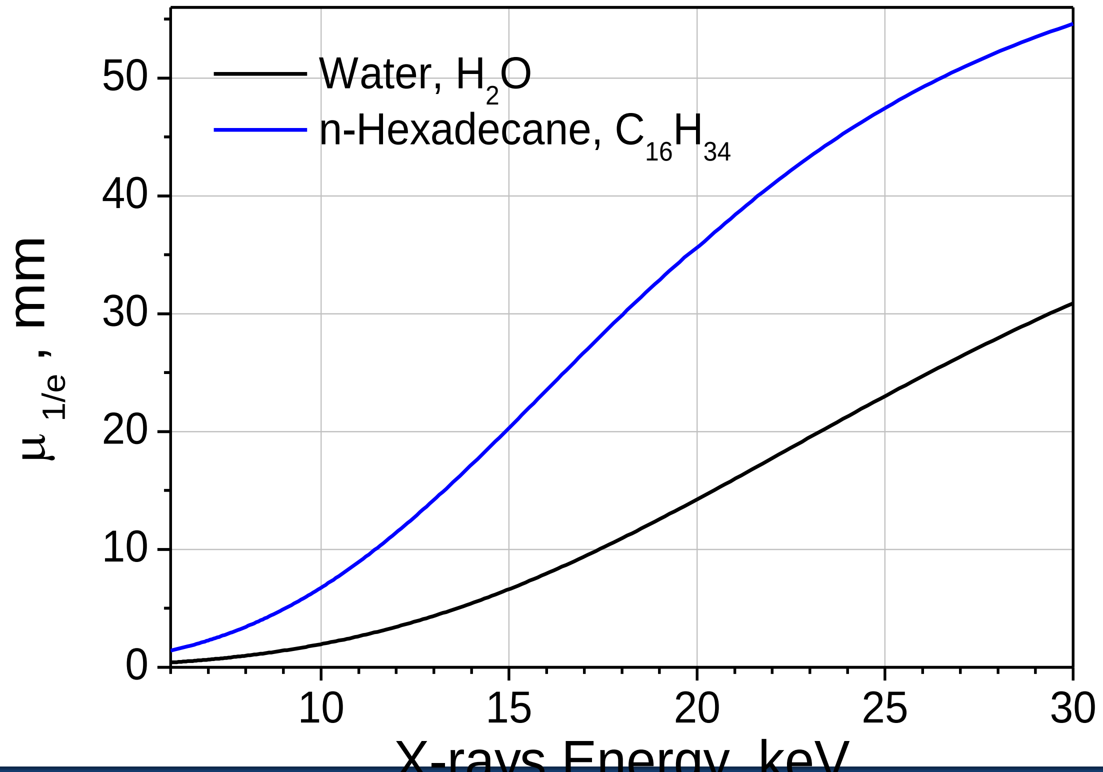

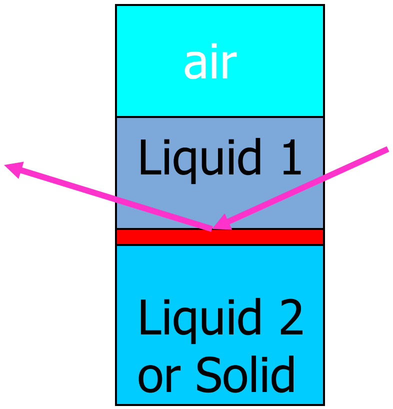

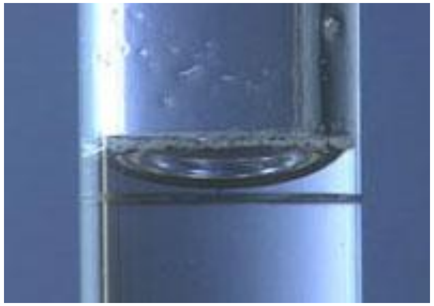

Nanoparticles as surfactants: contact angle & binding energy

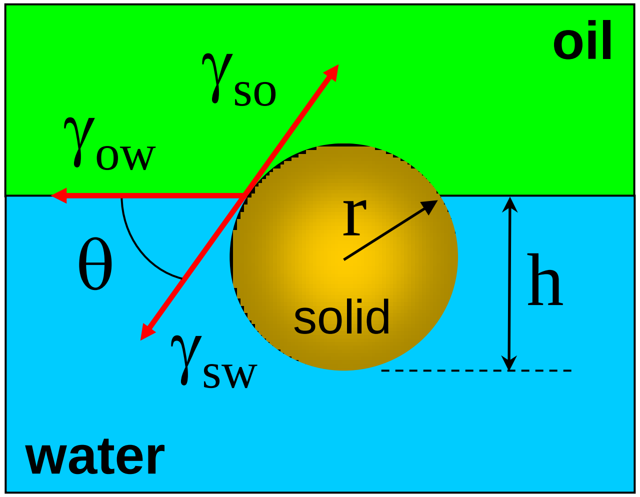

Particle immersion: $h = r(1+\cos\theta)$

Young's equation: $\gamma_{so} - \gamma_{sw} = \gamma_{ow}\cos\theta$

Solid-water contact area: $A_1 = 2\pi r h$

Missing oil-water area: $A_2 = \pi r^2 \sin^2\theta$

Binding energy: $\Delta E = A_1(\gamma_{so} - \gamma_{sw}) + A_2\gamma_{ow}$

$$\Delta E = \pi r^2[1 - |(\gamma_{sw} - \gamma_{so})/\gamma_{ow}|]^2 = \pi r^2\gamma_{ow}[1 - |\cos\theta|]^2 = \pi\gamma_{ow}h^2$$

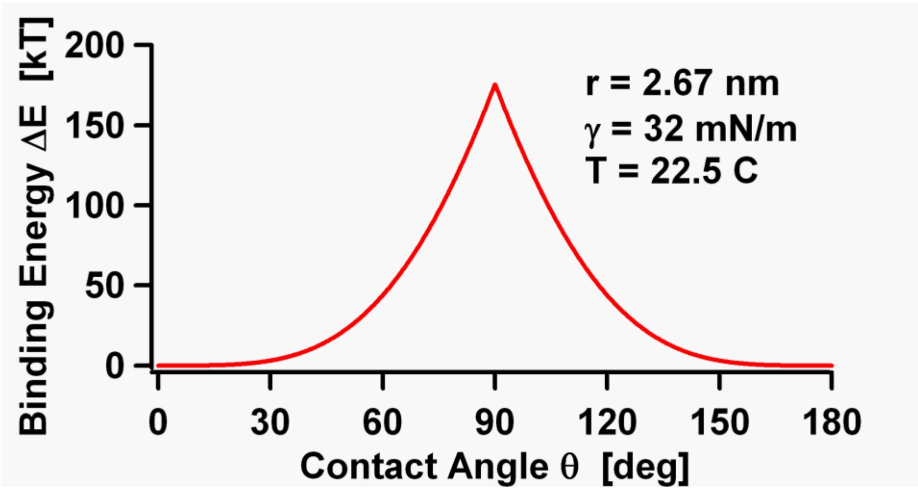

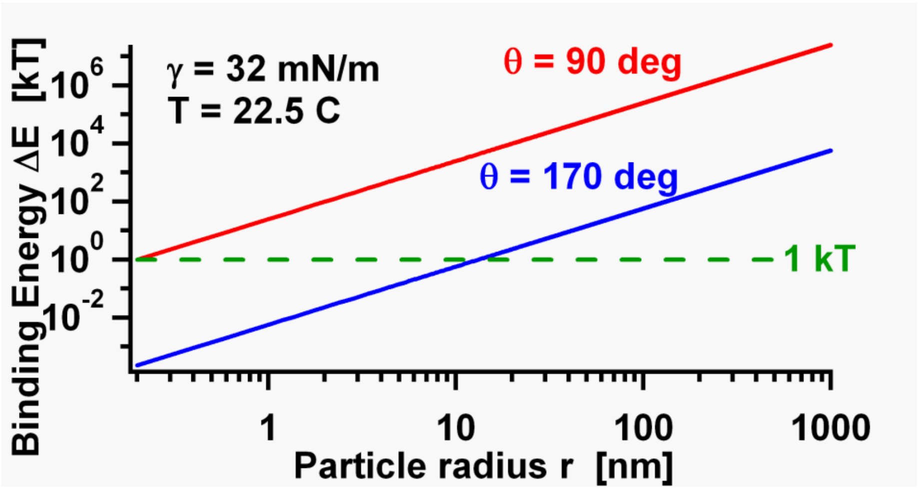

Langmuir Trough for Liquid-Liquid interface

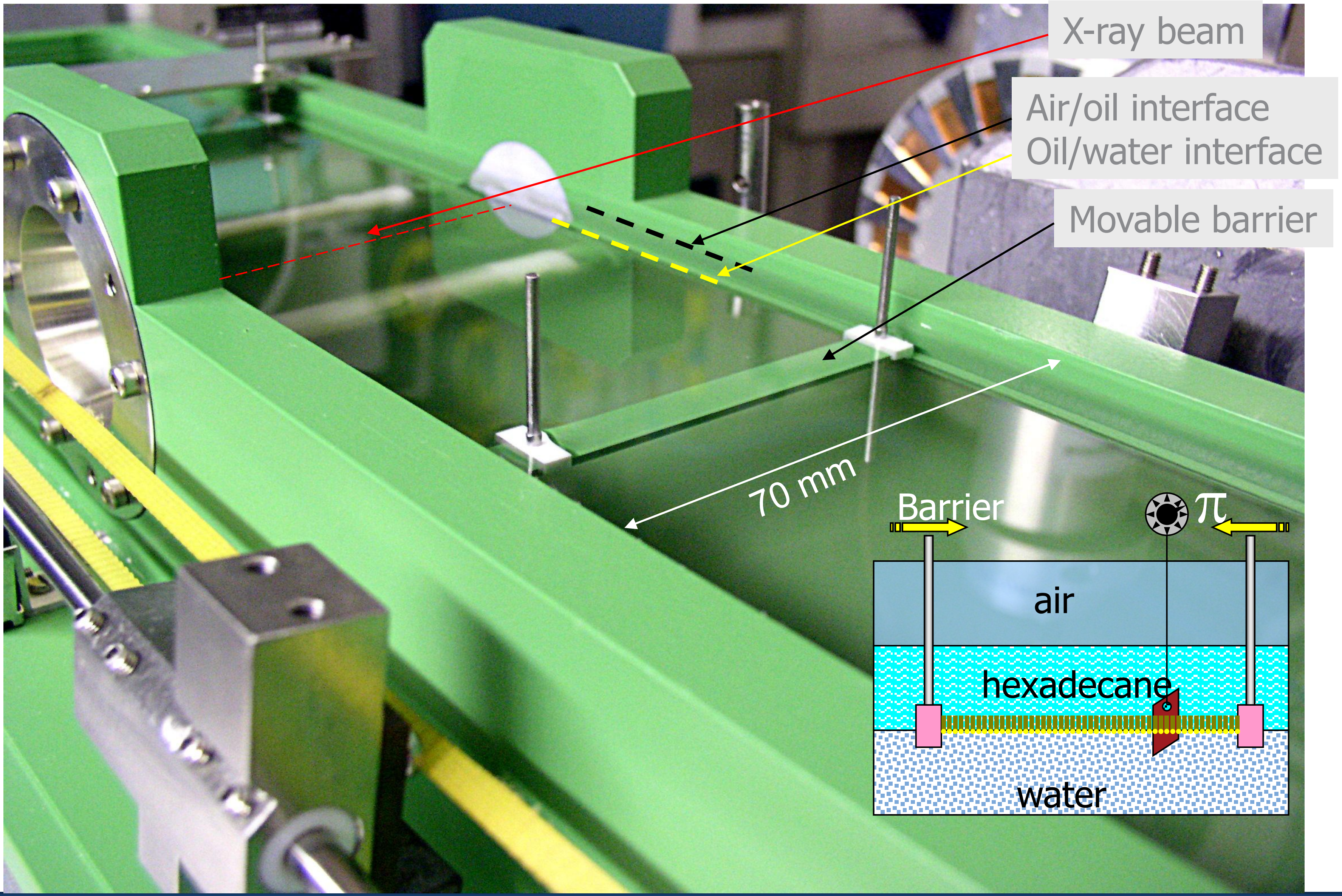

Formation and Ordering of Gold Nanoparticles at the Toluene-Water Interface

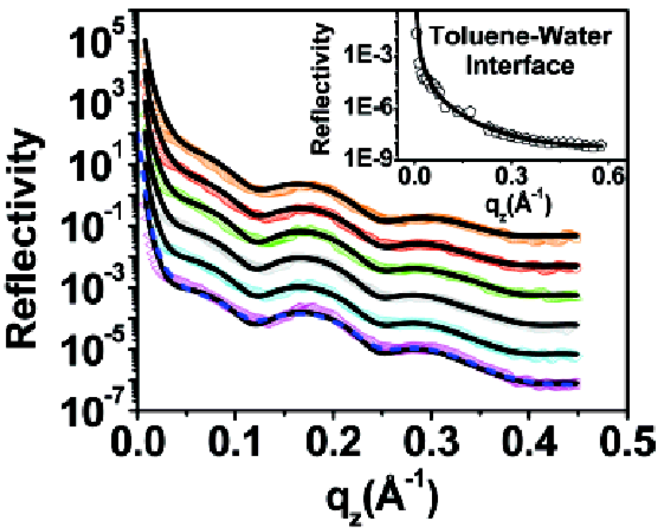

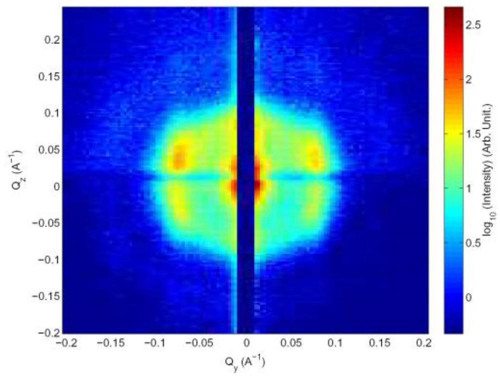

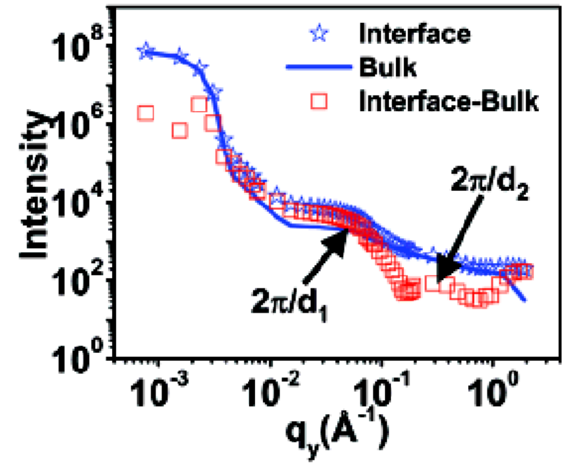

cluster-cluster separation d_1=180 Å

particle-particle separation d_2 = 34 Å

Each cluster consists of 13NPs with Ø 12 Å & 11 Å thick organic layer

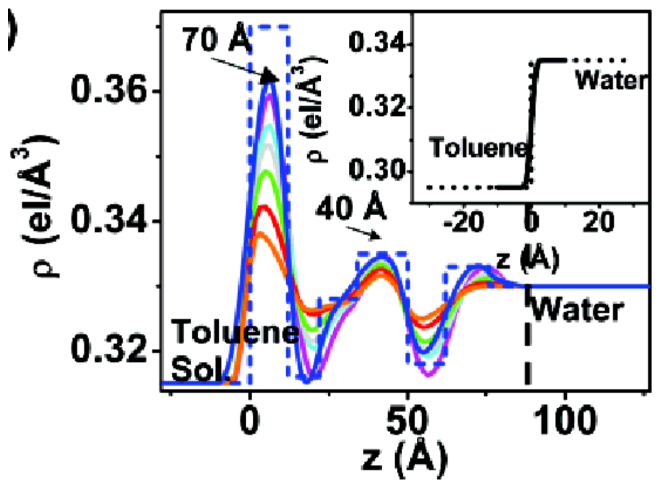

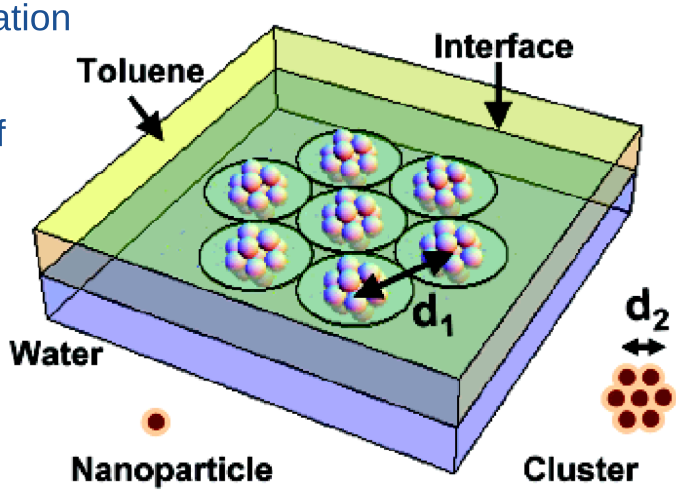

M.K. Sanyal et al., J. Phys. Chem. C, v. 112, 1739 (2008)

Bending Rigidity (κ) From GI Diffuse Scattering

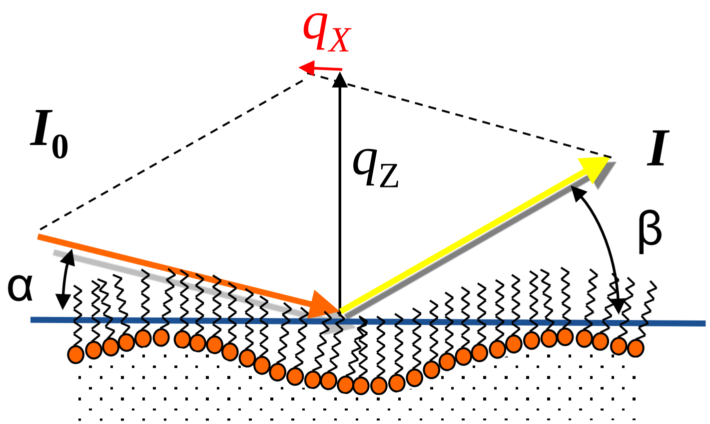

Capillary waves -> height fluctuation spectrum determided by
the surface energy (γ)
assocoated with the deformation modes (κ)
[Helfrich, Z. Naturforsch., 28c , 693, (1973)]

$$\left\langle z(q_{\parallel}) z(-q_{\parallel}) \right\rangle = \frac{1}{A} \frac{k_B T}{\Delta\rho g + \gamma q_{\parallel}^2 + \kappa q_{\parallel}^4}$$

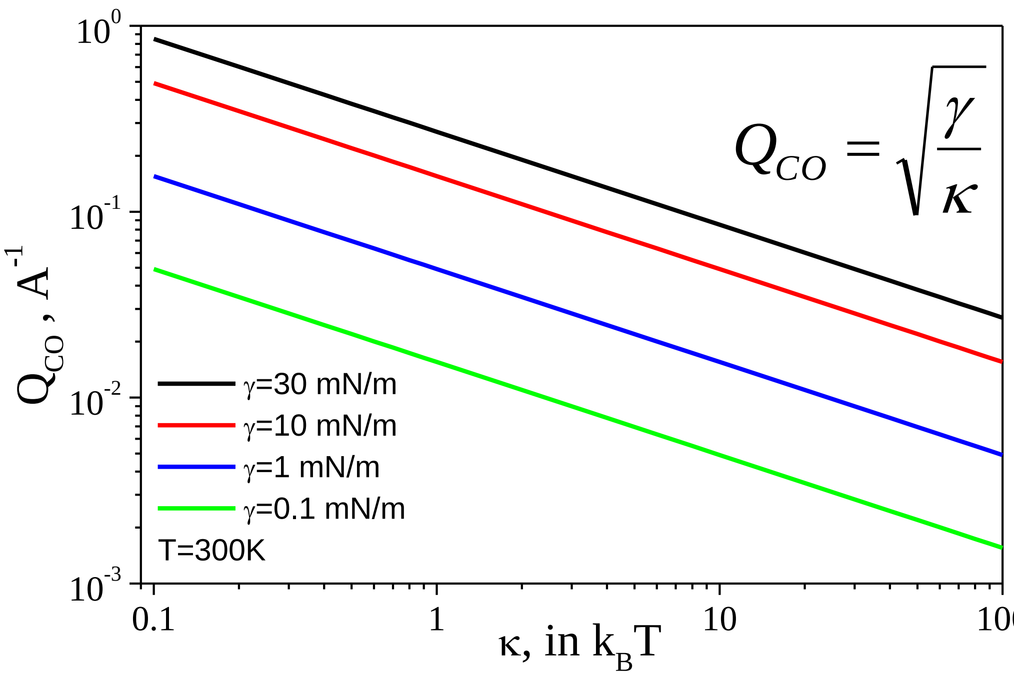

$$\frac{d\sigma}{d\Omega} \propto \left| t_{0,1}^{in} \right|^2 \left| t_{0,1}^{sc} \right|^2 \left| \tilde{\rho}(q_z) \right| e^{-q_z^2 < z^2 >} \times$$
$$\times \int d\, \mathrm{r}_{\parallel} \left(e^{q_z^2 < z(0) z(\mathrm{r}_{\parallel}) >} - 1 \right) e^{i\, \mathrm{q}_{\parallel} \mathrm{r}_{\parallel}}$$

S. Mora et al., Europhys. Lett., v. 66, p. 694 (2004)

Phospholipid monolayer at hexadecane water interface
Bending Rigidity (k)

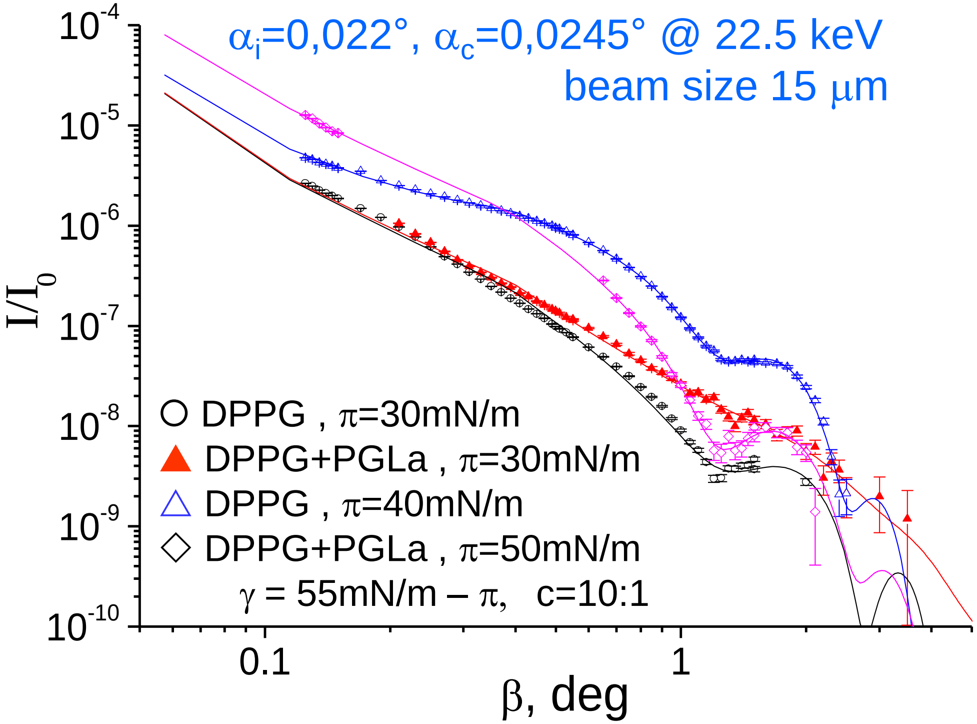

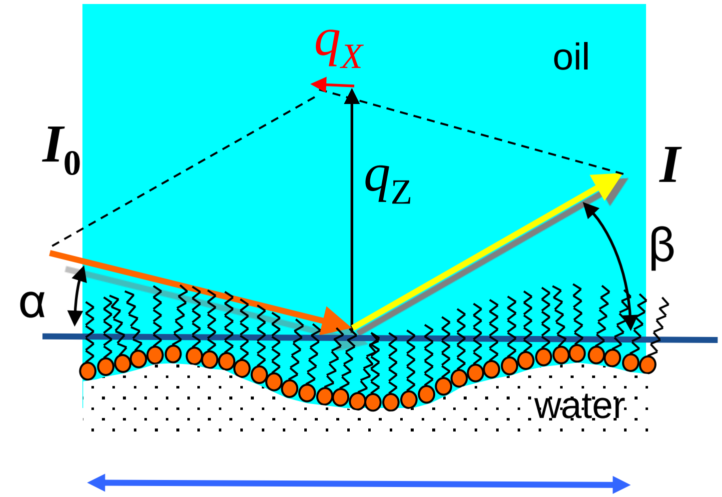

Beam travel path 70 mm

transmission ~20% (22keV)

	Rigidity κ (k_bT) @ π=30mN/m $\pi < \pi_c$	Rigidity κ (k_bT) @ π>40mN/m $\pi > \pi_c$
DPPG	55 ± 5	145 ± 5
DPPG+PGLa	27 ± 5	20 ± 5

Bending rigidity of the DPPG membrane decreses upon insertion of the antimicrobial peptide PGLa

E. Saint Martin et al., Thin Solid Films, v.515, p.5678, (2007)

X-ray Reflectivity + Fluorescence

Total Reflection X-Ray Fluorescence (TXRF)

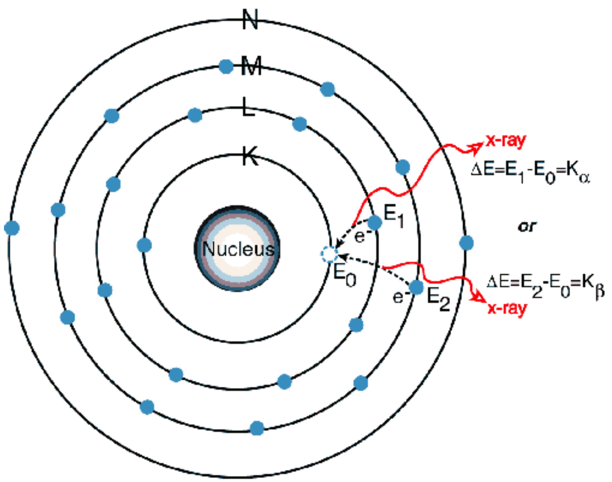

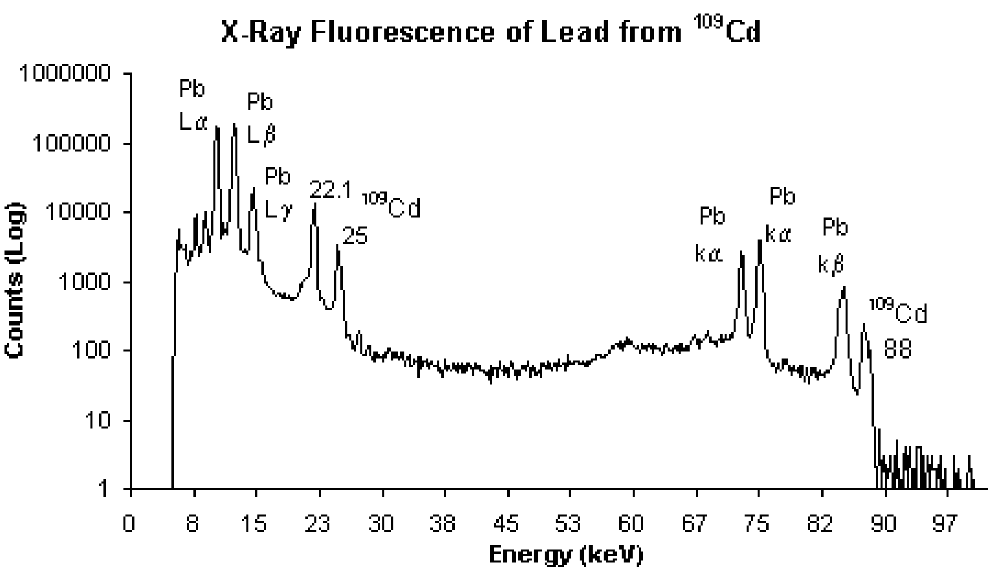

Specific ion adsorption and short-range interactions at the air aqueous solution interface

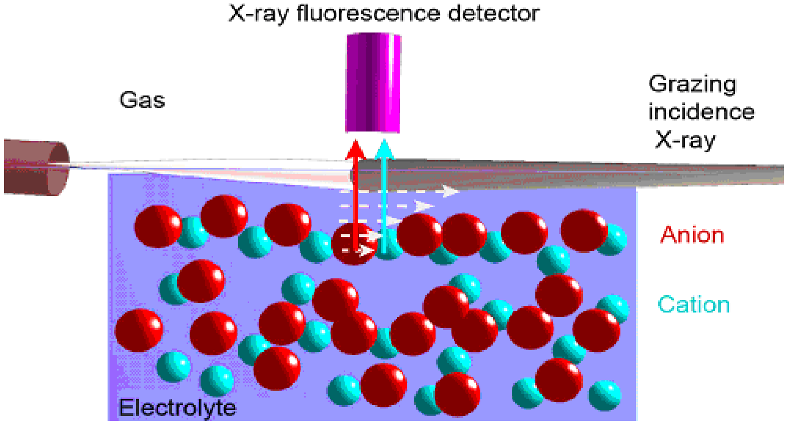

Concentration profiles

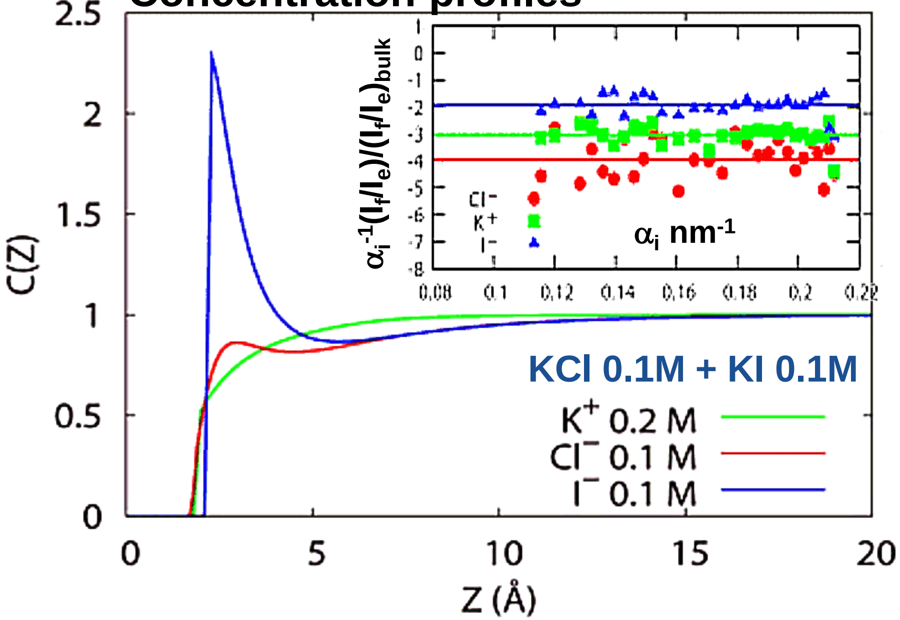

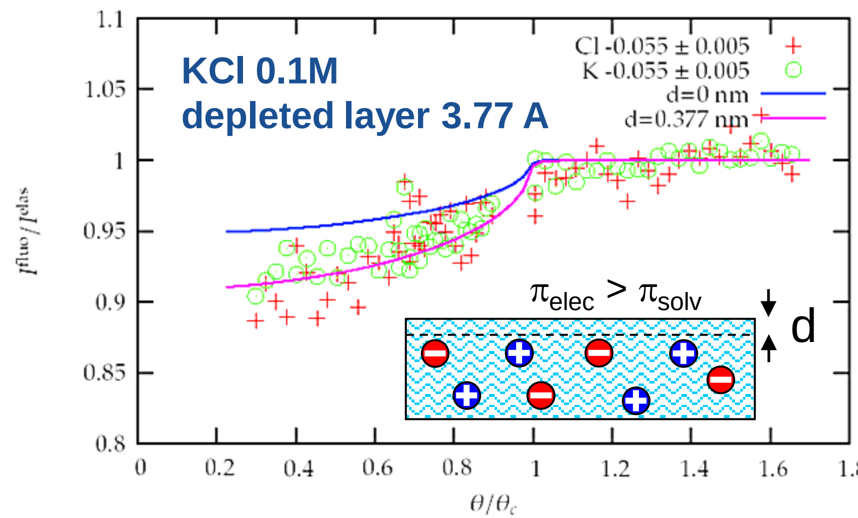

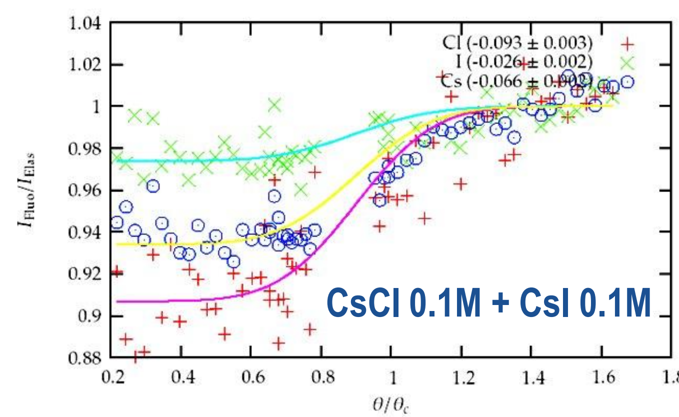

V. Padmanabhan et al., Phys. Rev. Lett. 99, 086105 (2007)

Semiconductor nano-structures. Quantum: dots, wires, crystals and molecules

size, shape, strain, chemical composition & spatial ordering

Free-standing $Si_{1-x}Ge_x$ nanoscale islands on Si(100)

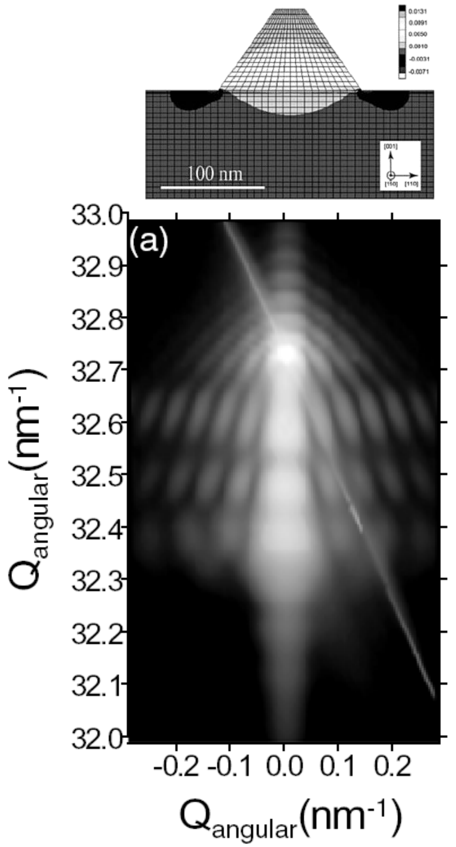

Three-Dimensional Si/Ge Quantum Dot Crystals

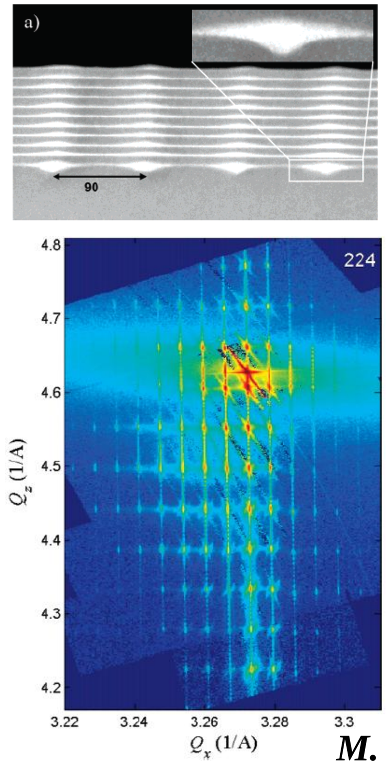

Hexapod-like (In,Ga)As/GaAs(001) quantum dot molecules

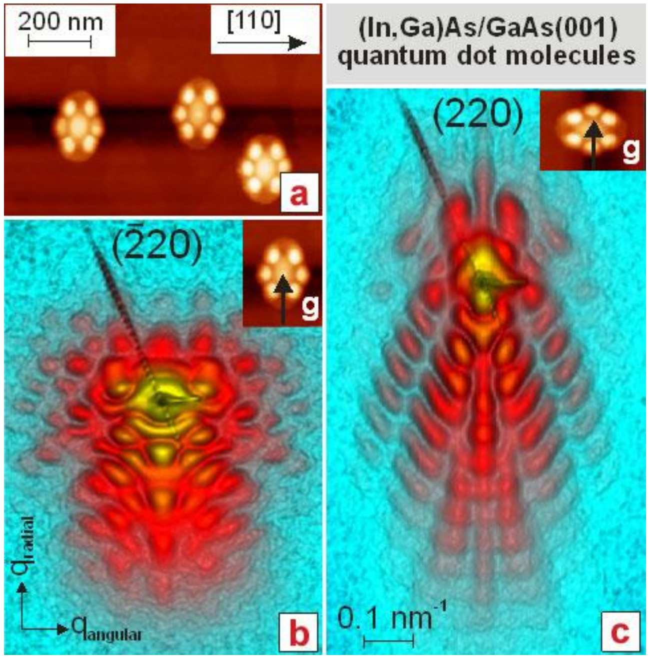

M. Hanke et al. Appl. Phys. Lett., v. 95, 023103, (2009)

D. Grützmacher et al., Nano Lett., Vol. 7, 3150, (2007)

D. Grigoriev et al., J. Phys. D: Appl. Phys., v. 36, A225-A230, (2003)

GENERAL VIEW OF EXPERIMENTAL HUTCH OF THE ID10B BEAMLINE AT ESRF

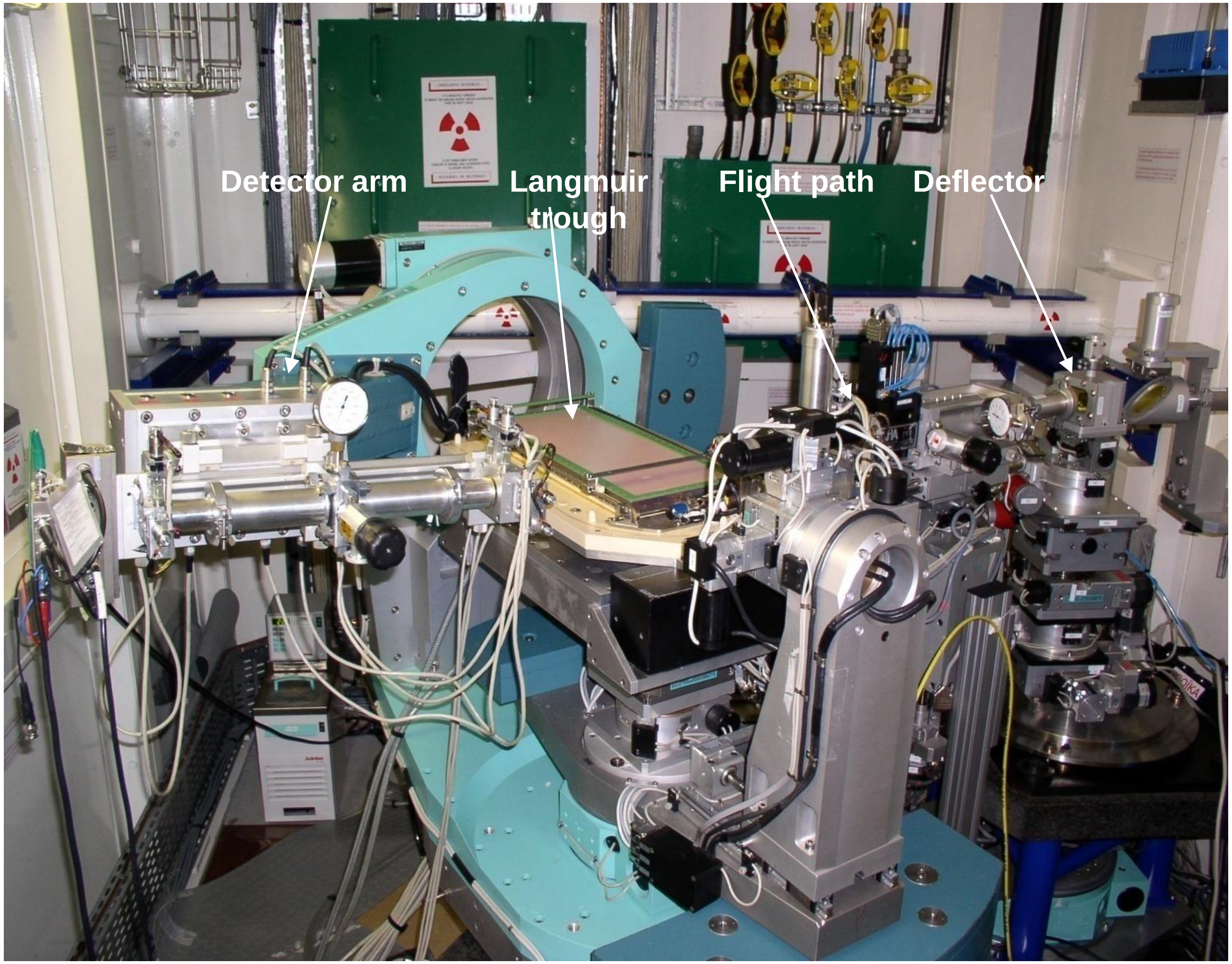

max beam size at sample 1×0.5 mm² (H×V) 44 m from the source
photon energy 7 keV < E < 30 keV (1.77 < λ < 0.41)
flux at sample: 10^{13} ph/s/mm² (at I=100 mA, E=9 keV)

The ID10B beamline is a multi-purpose, high-brilliance undulator beamline for high resolution X-ray scattering and surface diffraction on liquid and solid interfaces, combining grazing-incidence diffraction (GID), X-ray reflectivity (XRR), and grazing-incidence small-angle scattering (GISAXS) techniques in a single instrument. Scattering experiments can be performed in both horizontal and in vertical scattering geometry.

The beamline is optimized for experiments on liquid and fluid surfaces which are a particular specialty of the ID10B.

Scientific applications cover studies of the structural properties of soft and hard condensed matter materials.

Conclusion

X-ray surface sensitive technique is a powerful tool to study broad spectrum of science at surfaces and interfaces

Langmuir films

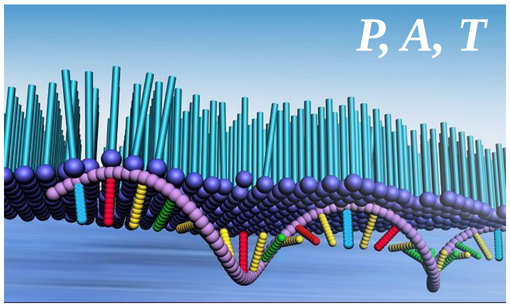

Elements distribution

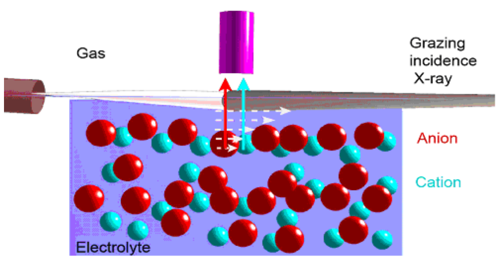

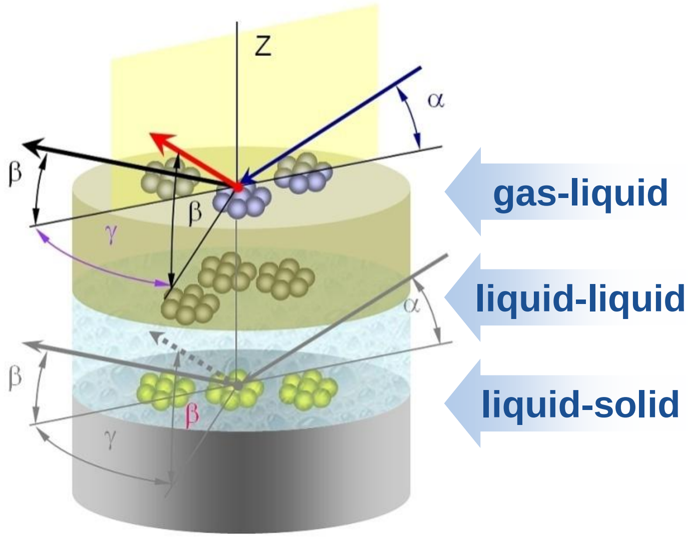

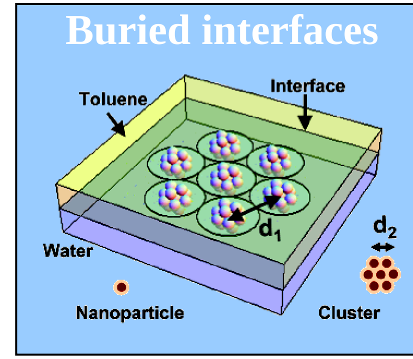

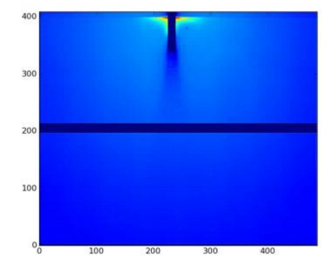

Complex fluids

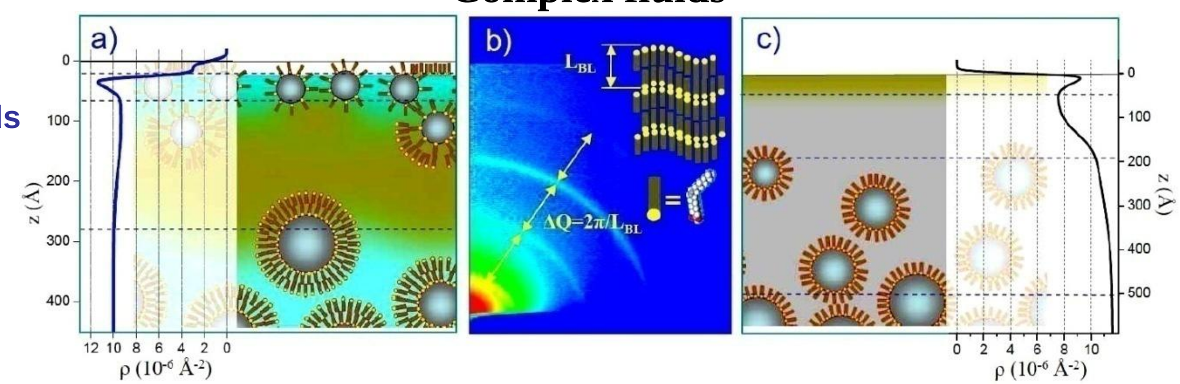

- Surface structure of simple and complex fluids
- Morphology and crystalline structure
  of thin organic and inorganic films
- 2D organization of molecules,
  macromolecules and nano particles
- Bio-mimetic systems & Bio-mineralization
- Chemistry & Electrochemistry
- Surfactants & ions ordering

Acknowledgments

ID10B & ESRF staff
A. Vorobiev

Numerous ID10B users

Thank you !

Further reading

J. Daillant & A. Gibaud, "X-Ray and Neutron Reflectivity: Principles and Applications", Springer, 1999

M. Tolan "X-Ray Scattering from Soft-Matter Thin Films" Springer, 1999

J. Als-Nielsen & D. McMorrow "Element of Modern X-ray Physics", John Wiley, 2001

I. K. Robinson and D. J. Tweet, Rept. Prog. Phys. 55, p.599 (1992)
J.Daillant, M.Alba, Rep. Prog. Phys. 63 (2000) 1725–1777

Grazing Incidence Scattering : Flux Requirements

$$I = \frac{I_0}{w_i h_i}\frac{d\sigma}{d\Omega}(q)\frac{w_d h_d}{L_d^2}$$

$$\frac{d\sigma}{d\Omega}(q) \sim r_e^2 \cos^2\psi \left|t_\alpha\right|^2 \left|t_\beta\right|^2 {}_\Delta\rho_e^2 A_\parallel \frac{k_B T}{\gamma q_\parallel^2}$$

$\gamma = 72\cdot 10^{-3}\ N/m$ $\qquad w_i = w_c = w_d = h_d = 3\cdot 10^{-4}\ m$

$r_e = 2.8\cdot 10^{-15}\ m$ $\qquad h_i = 10^{-4}\ m \qquad L_d = 0.5\,m$

$\rho_{H2O} = 3.3\cdot 10^{29}\ el/m^3$ $\qquad q_\parallel = 10^9\ m^{-1}$

$\cos^2\psi \left|t_\alpha\right|^2\left|t_\beta\right|^2 \sim 1$ $\qquad A_\parallel \sim \frac{w_i w_c}{\sin\psi} = 3.6\cdot 10^{-6} m^2$

$$\frac{d\sigma}{d\Omega}(q) \sim A_\parallel \times 5\cdot 10^{-8}$$

$$\frac{d\sigma}{d\Omega}(q) \sim 2\cdot 10^{-13}$$

$$I \sim I_0 \cdot 2\cdot 10^{-12}$$

$$I_{Sollers} \sim I_0 \cdot 4\cdot 10^{-11}$$

for 3% *error bar* $N \sim 10^3$
& 60 sec *counting time*

$$I_0 \sim 4\cdot 10^{11}\ ph/s$$